Master of Science Thesis in Electrical Engineering
Department of Electrical Engineering, Linköping University, 2018

Turbo Heat Transfer Modelling for Control

John Lundqvist, Anton Nordlöf

LINKÖPING UNIVERSITY

Master of Science Thesis in Electrical Engineering

Turbo Heat Transfer Modelling for Control

John Lundqvist, Anton Nordlöf

LiTH-ISY-EX--18/5139--SE

Supervisor: **Ph.D. Student Robin Holmbom**
ISY, Linköpings universitet
Patrik Martinsson
Volvo Car Corporation

Examiner: **Professor Lars Eriksson**
ISY, Linköpings universitet

Division of Automatic Control
Department of Electrical Engineering
Linköping University
SE-581 83 Linköping, Sweden

Abstract

The demand for lower emission engines forces the car industry to build more efficient engines. Turbocharged engines are on the rise, and better understanding of the heat transfer and efficiency of the turbocharger is needed to build better ones. A lot is known about the overall efficiency of the turbocharger, but not much is known about where the heat losses are located and how they interact with each other.

This thesis presents a one dimensional model for heat exchange in the turbocharger and investigates how the heat flows from the hot exhaust gases to the cold intake air. Data is gathered by performing tests on a single scroll turbocharger in an engine test bench at Linköping University. The tests are focused on operating points where the air mass flow is low and neither the compressor nor the turbine works adiabatically.

The results show that it is possible to estimate the heat flows together with the efficiency of the turbine and compressor using only known parameters, eliminating the need to add any new sensors to the engine.

Acknowledgements

We would like to thank all the people that helped us during the creation of this report. Thank you Lars Eriksson for giving us this master thesis to work on. Thanks to Patrik Martinsson and the team at Volvo Car for the opportunity to do this thesis and helping us with problems big and small.

Robin Holmbom should have an extra big thank you for all the supervision, support and constant answering to our dumb questions. Thanks also to Tobias Lindell for helping us in the lab and making sure that we did not destroy all the hardware.

Last but not least we want to thank our co master thesis writers in room 3C:509 for all the laughs and curvefever.io games (there were a few), without you it would not have been half as fun.

Contents

Nomenclature

Dimensionless

ϵ	Emissitivity
η	Efficiency
γ	Specific heat ratio
C_d	Drag coefficient
Nu	Nusselt number
Pr	Prandtl number
Re	Reynolds number

Other

$\dot{m}$	Mass flow	$[kg/s]$
μ	Dynamic viscosity	$[kg/ms]$
ρ	Density	$[kg/m^3]$
σ	Stefan Boltzmanns constant	$[W/m^2K^4]$
A	Area	$[m^2]$
C_p	Specific heat capacity	$[J/kgK]$
g	Gravitational constant	$[m/s^2]$
H	Enthalpy	$[J]$
h	Heat transfer coefficient	$[W/m^2K]$
k	Thermal conductivity	$[W/m^2K]$
R	Specific gas constant	$[J/kgK]$

T	Temperature	$[K]$
u	Velocity	$[m/s]$
v	Kinematic viscosity	$[m^2/s]$
W	Power	$[W]$
$\dot{Q}$	Heat flow	$[W]$

1 Introduction

In this chapter the background to why this thesis is written is explained along with the goal and expected outcome of the thesis.

1.1 Background

With tightening demands on emissions and an increasing market demand for more fuel efficient engines the main challenge for today's automotive engineers is to make engines more fuel efficient without losing power. One main step in making fuel efficient engines is to downsize. To keep the power and torque whilst reducing the engine displacement, forced induction is often used in the form of a turbocharger. The turbocharger increases the amount of oxygen forced into the combustion chamber, increasing the amount of fuel burnt per revolution and thus the power output of the engine. This thesis is part of a joint research project between Volvo Car Corporation and Linköping University.

1.2 Purpose and goal

With the turbocharger comes the need of wastegate control, the valve, that if open, makes the exhaust gases bypass the turbine, essential to keep the pressure at manageable levels. The amount of gas flow through the wastegate at any given position is however not known. With better understanding of these dynamics it can be possible to create better turbo control models thus increasing the overall efficiency of the combustion engine.

Another problem is the heat transfers that occurs across the turbocharger. The losses from the turbocharger is well known, but where the losses occur within the system is not well documented.

The purpose of this thesis is mainly to widen the technical expertise on the subject of turbocharger models. To achieve good control and understanding of the turbocharger the models have to accurately describe the different effects in the turbine and compressor. Earlier models do not include the heat transfer from the warm turbine side to the cooler compressor. This often results in an overestimation of the compressor's thermodynamic effectiveness. The heat flux generated in the turbocharger depends on many parameters that in themselves are difficult to estimate.

The work done by Storm (2017) and Vilhelmsson (2017) that dealt with heat transfer in the turbine and pulsating mass flow were the basis of this thesis.

The goal were to extend these models to include heat transfer in the bearing housing and compressor, as well as describing the mass flow that goes through the turbine and wastegate to allow better control models.

1.3 Problem formulation

To be able to generate a good model of the turbocharger, many unknown parameters needs to be known. One of the main problems with the turbocharger is the generated heat in the turbine because of hot exhaust gases. Components in the vicinity of the turbine that are cooler will generate a heat flux from hot to cold in an attempt to reach thermal equilibrium. In today's Volvo engines the performance is mapped in a test bench and the losses across the turbine is lumped together as a lump sum.

Better knowledge to where the losses occur could help improve the control of the engine. Earlier work regarding the heat transfer effects has been done by Storm (2017). That work only considered the heat transfer in the turbine, not the heat transfer in the bearing housing and the compressor which this thesis have investigated.

Problems also occur when the mass flow into the turbine and wastegate are estimated. Since the outlet of both the gas flow from the turbine and the wastegate is combined in the turbine outlet there is a big problem being able to measure how much of the flow that is actually going through the wastegate at any given position. With a pneumatically controlled wastegate the opening of the wastegate is not known. However by changing to an electrical servo for wastegate control, the position of the servo is known and can be regulated with desired accuracy.

1.4 Delimitations

This thesis relies partly on reused data from already performed tests performed both at VCC and at Vehicular Systems at Linköping University. Additional data was collected by performing engine tests at Vehicular Systems. Some desired measurements were not feasible to do due to different limitations of the hardware, such as removal of water coolant. Only one type of turbocharger was investigated, a single turbo system provided by VCC which was tested at steady state conditions.

1.5 Risk analysis

During the work of the thesis it was important to identify and be aware of conditions that may have had an impact on the credibility of the end result. Things that affect measurements, and simplifications in theory, can be some of the factors that impact the end result in an undesirable way.

1.5.1 Sensors

One of the issues regarding the sensors, especially the temperature sensors, are the measured quantities. Temperature readings are difficult to isolate and determine. As an example, a sensor that is supposed to measure gas temperature in the exhaust manifold could have been corrupted by conduction as well as radiation from the manifold wall. One big source of error could also have been positioning of the sensors and other mounting errors that may have given undesired or irrelevant readings.

Redundancy is another issue that could have been a problem, if only one sensor were measuring one quantity, no data would have been available to collect if that particular sensor were damaged or broken. One temperature sensor with very low time constant could have been used to measure the pulsating temperature in the exhaust manifold, due to the delicate electronics the lifespan of this sensor may have caused some trouble, it might have broken before any significant data were collected.

1.5.2 Other

One of the delimitations of this work are the steady state measurements. All models are based on steady state operating points. Since the turbocharger in a combustion engine often are exposed to transient conditions, together with the thermal inertia, it could result in the models to be insufficient.

The biggest delimitation was time, there were a few time consuming activities that needed to be addressed. First of all was the lead time for the turbocharger preparations, sensors needed to be installed on the turbocharger as well as transported to the engine lab at Linköping University, this was delayed by 5 weeks. The gas stand at VCC in Gothenburg was fully booked which meant that the desired tests could not be done.

1.6 Outline

Section 1, Introduction
Background, Purpose and goal, Problem formulation, Delimitations.
Section 2, Related research
State of the art, Expected results, Risk analysis.
Section 3, Theory
Theory used in calculation of the model. Including thermodynamics, heat transfer and flow theory.
Section 4, Models
Models used and how to calculate the models from measurement data.
Section 5, Measurements
The test setup, method, and hardware is described.
Section 6, Results
Presentation of and analysis of the results.
Section 7, Discussion
The results, models, and work process is discussed and analyzed.
Section 8, Conclusions
Concluding thoughts and future work.

2

Related research

Many previous studies and research, function as inspiration and a foundation to build upon with this master thesis. The most important ones are presented and discussed in this section.

2.1 State of the art

The state of the art is divided into two categories depending on the problem. The first is *Turbocharger heat transfer* which investigates earlier work regarding the different heat mechanisms that is occurring in the turbocharger.

The second is *Dynamic pulsating flow* which investigates work done regarding the problem of describing flow during transients or static that are pulsating.

2.1.1 Turbocharger heat transfer

A turbocharger consists of mainly three different parts. The turbine, compressor and the bearing housing. Since the turbine exhaust gas temperatures could reach up to 900°C, and the range for the compressed air, water cooling and oil are well below such temperatures, heat transfer across the turbocharger is inevitable (Aghaali et al., 2015). If the heat transfer was to be neglected in the turbocharger the estimated efficiency of the turbine and compressor could be wrong (overrated and underrated). According to Sirakov and Casey (2013) conventional turbo maps could underestimate the compressor and overestimate the efficiency up to 20 % at low speeds. The reason why is because heat from the turbine could heat up the intake air in the compressor (Storm, 2017), and the turbocharger efficiency often is calculated using change in enthalpy or temperature over the comopressor. (Eriksson and Nielsen, 2014; Nguyen-Schäfer, 2016; Romagnoli and Martinez-Botas, 2009).

There are several heat transfer mechanisms in the turbocharger that affects the heat flux across the turbocharger, the contributors are convection, conduction, and radiation.

In Baines et al. (2010) the internal heat transfer only takes convection and conduction into consideration because radiation is assumed to be negligent in the turbine and compressor. Also, the heat transfers with the greatest magnitude and significance in the engine is said to be the external heat transfer from the turbine to the environment, and the internal heat transfer from the turbine to the bearing housing. Serrano et al. (2010) did not take radiation into consideration when their turbocharger heat transfer model were developed, but unlike Baines et al. (2010) it was claimed to be necessary to study in future work. Romagnoli and Martinez-Botas (2009) suggests that the engine has a noticeable effect on compressor temperature, therefore it is suggested to include the heat flux generated from the engine in the model. Also, it was concluded that there is a linear relation between the exhaust gas temperature and the bearing housing.

In Serrano et al. (2015) the importance of predicting the heat transfer during low loads (i.e. low N_t) is stressed. During high loads the total enthalpy drop over the turbine consists of almost only mechanical power in some cases. The same article mentions that during medium to low engine loads the compressed air absorbs energy from the compressor casing because the oil coolant is hotter than the compressor outlet air. During high compressor loads the process is reversed, the compressor outlet air becomes hotter than the oil coolant and the heat is transferred from the air to the oil. Although, it is shown that during high loads the heat transfer effects in the compressor is negligible and the compressor behaves almost adiabatic. Similar conclusions are made by Bohn et al. (2005) that concluded for small Reynolds numbers, the compressor air is heated by the heat flux from the turbine. During high Reynolds numbers the air is heated by the compression rather than by the turbine. Similar conclusions are also made by Sirakov and Casey (2013) and Tanda et al. (2017).

In Aghaali et al. (2015) several tests were conducted to determine the heat transfer effects of different parts of the turbocharger, such as water cooling, external ventilation with a fan and a radiation shield between the turbine and the compressor. It were concluded that the radiation shield has no significant impact of the energy balance of the turbocharger. The water cooling has a bigger impact, especially regarding the internal heat transfer from the bearing housing to the compressor, as well as the external heat transfer from the bearing housing.

Romagnoli and Martinez-Botas (2012) finds that the surface temperature of the turbine and compressor surface were proportional to the temperature of the exhaust gases. They also found that the surface temperature of the bearing housing were varying consistently with the oil coolant temperature with a difference of about $30K$. Even though the flow conditions are different they find strong agreement in results, showing that sensor location and quality is a dominant factor and therefore need careful planning. With pulsating flow the change of mass flow in the turbine gives a pulsating Reynolds number that needs to be accounted for in simulation.

Payri et al. (2014) states that the most important external heat flux comes from

the turbine housing. One negligible external heat flux is the bearing housing if compared to the turbine enthalpy drop.

In Aghaali and Angstrom (2012) the uncertainty of the exhaust gas temperatures mentioned, because of pulsating flow and big temperature gradient of the exhaust gases the thermal sensors are too slow to measure the temperature in high resolution.

2.1.2 Lumped capacitance method

The work done in Storm (2017) utilizes the lumped capacitance method to model the heat transfer in the turbine. Burke et al. (2014), Cormerais et al. (2009) and Olmeda et al. (2013) amongst others have also used this method. The general idea of the method is to create several thermal nodes that are connected together with conduction, convection and radiation. Burke et al. (2015) used lumped capacity modelling and found that at least 20 % of the enthalpy change in the turbine is due to heat transfer in the turbine. During low speeds where the power operating conditions are low the heat transfer contributes significantly more to the change in enthalpy compared to during high speeds.

2.1.3 Dynamic pulsating flow

The gas flow through the turbine is complex and hard to model without simplifications. The turbine inlet/outlet can be seen as short pipes with constant diameter making the flow quite consistent through these parts. Past the scroll and stator/rotor the flow of gas is much more complex. The diameter of the scroll is gradually reducing and when the gas enters the rotor flow passages the mass flow is not constant. With large spatial variations the Reynolds numbers will not be the same in all parts of the turbine which will be hard to model and are even harder to validate. Therefore the model is simplified by assuming the whole turbine side of the turbo consists of just two pipes, each with a constant diameter Burke et al. (2015).

The assumption that the turbine flow can be modelled as flow through pipes with constant diameters and an adiabatic expansion between them enables the heat transfer in the pipes to be calculated using Newtons law of cooling. The Reynolds number is defined for the whole turbine stage and can be estimated based on measurements of temperature and mass flow. With the gas stand the flow is constant and the Reynolds number can be considered both statically and time averaged. However during the pulsating flow that occurs with the combustion engine, mass flow and temperature of the gas is fluctuating over time and with it the Reynolds number. In Burke et al. (2015) the pulsating Reynolds number are included in the heat flow model.

One factor that can influence the dynamic heat flow is that the specific heat ratio, γ is changing with both temperature and gas mixture. While Vilhelmsson (2017) looks at the compressor side and therefore uses $\gamma_{air} = 1.4$, the standard for air in room temperature. In this paper the focus will be at the turbine side and a model of the flow through the wastegate. The gas flowing through turbine

side however is a burnt mixture of air and gasoline at a temperature up to 900°C and thus have a different specific heat ratio from that of air in room temperature.

There are several ways of calculating the specific heat ratio. In Klein (2004) three models are estimated, linear scaling with temperature, polynomial model based on Kreiger and Borman's polynomial model of the internal energy, u and lastly using a Matlab package called Chepp (ISY, 2018). The modelling of γ for exhaust gases using Chepp is the most exact, and for temperatures below 1700°C the polynomial approach is also of comparable precision. They both give much better results than the standard linear scaling.

3

Theory

In this section the basic theory is explained. Thermodynamics, heat transfer and isentropic flow are the key theories in this thesis.

3.1 Thermodynamics

A simplified definition of thermodynamics are explained as the state of the matter and the energy transport, work, and heat associated with the change of state (Storck et al., 2012).

The first law of Thermodynamics for an open system

An open system is defined as a predetermined area where mass, work, and heat are allowed to flow across the boundaries of the system. The first law of Thermodynamics applied on an open system control volume is given by,

$$\dot{Q}_{12} + \sum \dot{m}_1 \left(H_1 + \tfrac{1}{2} u_1^2 + g z_1 \right) = \frac{dE_{cv}}{dt} + \sum \dot{m}_2 \left(H_2 + \tfrac{1}{2} u_2^2 + g z_2 \right) + W_t \qquad (3.1)$$

The open system control volume are shown in Figure 3.1. If the open system is in steady state, i.e the mass flow and energy content is constant, it could instead be written as,

$$(\dot{Q}_1 - \dot{Q}_2) = \dot{m}(H_2 - H_1) + \tfrac{1}{2}\dot{m}(u_2^2 - u_1^2) + \dot{m}g(z_2 - z_1) + (W_2 - W_1) \qquad (3.2)$$

Equation (3.2) can be rewritten if the change in kinetic energy and potential energy is assumed to be negligible, and that the enthalpy are replaced as temperature and specific heat capacity. The resulting equation is given by,

$$(\dot{Q}_1 - \dot{Q}_2) = \dot{m} C_p (T_2 - T_1) + (W_2 - W_1) \tag{3.3}$$

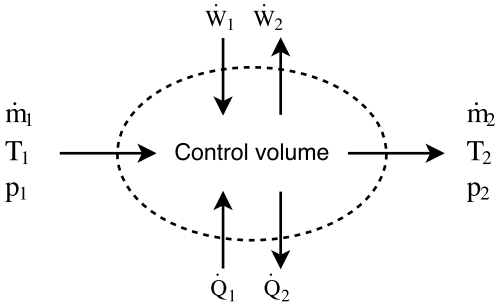

Figure 3.1: *The first law of thermodynamics illustrated by an open system control volume.*

3.1.1 Heat transfer

There are three different ways heat can be transferred, by convection, conduction and radiation.

Convection

When a solid surface and an adjacent fluid in motion is transferring energy it is called convection, its a result of conduction and the motion of the fluid (Cengel et al., 2017). There are two types of convection, natural and forced. Natural convection occurs when there are heat differences in the fluid which creates a flow. Forced convection occurs when external sources influences the fluid, such as fans or pumps. The expression to describe convection is *newtons law of cooling* and is given in equation (3.4). h_{conv} is the *convection heat transfer coefficient*, A_s is the surface area, T_s is the surface temperature and T_∞ is the fluid temperature.

$$\dot{Q}_{conv} = h_{conv} A_s (T_s - T_\infty) \tag{3.4}$$

Conduction

Conduction is the transfer of heat in solid materials, fluids and gases. It is usually associated with heat transfer in solid materials, but in fluids and gases the effects of conduction is included in the convection. (Storck et al., 2012). Fourier's law for a stationary and one-dimensional heat transfer in a flat and isotropic wall gives a linear relation of temperature change across the wall. Locally, the expression is given by equation (3.5). k is the thermal conductivity of the solid, A is the wall area.

$$\dot{Q}_y = -kA \frac{\partial T}{\partial y} \tag{3.5}$$

Radiation

The last mean of heat transfer is radiation. An exchange of electromagnetic radiation between the wavelengths of $0.1\mu m$ and $100\mu m$ is what enables the heat transfer Storck et al. (2012) . The property that decides how efficient a material can emit thermal radiation is the *emissivity* and is given by ϵ. It's a function of both surface temperature and radiation wavelength, but some materials have constant emissivity. The emitted heat from a surface is given by the expression in equation (3.6) where $\sigma = 5.67 \cdot 10^{-8}$ $[W/m^2K^4]$ is the Stefan-Boltzmanns constant.

$$\dot{Q} = \sigma \epsilon A T^4 \tag{3.6}$$

The radiation heat exchange between two bodies is expressed by (3.7). ϵ_{12} is the resulting emissivity.

$$\dot{Q} = \sigma \epsilon_{12} A (T_1^4 - T_2^4) \tag{3.7}$$

3.1.2 Isentropic flow

The turbine scroll and wastegate opening can be viewed as a converging nozzle leading to an expanding body. This enables the flow through the wastegate and turbine to be calculated using theory for isentropic flow through nozzles. When the exit speed of the gas reaches supersonic speeds, Mach one, the flow becomes choked. When choked flow is reached only an increasing upstream pressure can increase the mass flow through the choke point. With choked flow no information can travel upstream in the gas. This is important because during choked conditions the mass flow rate can be calculated to only depend on the temperature and the pressure drop over the nozzle. Assuming choked flow the mass flow rate can be described by,

$$\dot{m} = C_d A \sqrt{\gamma \rho_0 P_0 \left(\frac{2}{\gamma + 1} \right)^{\frac{\gamma+1}{\gamma-1}}} \tag{3.8}$$

where C_d is the discharge coefficient, A is the discharge hole cross-sectional area, P_0 the absolute upstream total pressure of the gas, ρ_0 is the gas density at absolute pressure and temperature and γ is the specific heat ratio for the gas. According to Holmbom and Eriksson (2018), *Ohata's Compressible Flow Model* are comparable to more complex models when it comes to estimating mass flow from flow bench measurements, this is the reason why this thesis uses Ohata's model. The model utilizes conservation of mass, energy, and momentum. The following equations give Ohata's model:

$$\dot{m} = \frac{p_1}{\sqrt{RT_1}} A_{eff}(\alpha)\Psi_{cv} \tag{3.9}$$

$$\Psi_{cv}(\Pi) = \sqrt{\frac{\gamma+1}{2\gamma}(1-\Pi)\left(\Pi + \frac{\gamma-1}{\gamma+1}\right)} \tag{3.10}$$

$$\Pi = \begin{cases} \frac{p_2}{p_1}, & if \quad \frac{p_2}{p_1} \geq \frac{1}{\gamma+1} \\ \frac{1}{\gamma+1}, & otherwise \end{cases} \tag{3.11}$$

where R is the specific gas constant, and $A_{eff}(\alpha) = C_d A$ is the effective area that depends on the wastegate opening.

3.1.3 Compression

If the compression of air are assumed to be adiabatic, with no heat transfer to or from the gas during compression, the temperature can be calculated as

$$T_{2,adi} = T_1 \left(\frac{p_2}{p_1}\right)^{\frac{\gamma-1}{\gamma}} \tag{3.12}$$

where $T_{2,adi}$, p_2 is the temperature and pressure after the adiabatic compression, and T_1, p_1 is the upstream temperature and pressure. The specific heat ratio, γ for air is 1.4 at 20°C. The specific work can then be calculated as

$$W_{c,adi} = \frac{R(T_2 - T_1)}{n-1} \tag{3.13}$$

where for an adiabatic process the constant n is equal to γ.

In the compressor, heat flow to the gas can not be ignored, so the effect can then be described by the first law of thermodynamics,

$$W_c + \dot{Q} = \dot{m}_c c_p (T_2 - T_1) \tag{3.14}$$

3.1.4 Heat transfer by Nusselt, Prandtl, and Reynolds

To calculate the heat transfer by convection from the the compressor wall to the air a theoretical approach is possible by using dimensionless numbers as shown in Serrano et al. (2015). The heat transfer is described as

$$\dot{Q}_{conv_{ch\to c}} = \overline{Nu}_{ch\to c} k \pi L_{char} \left(T_{ch} - \frac{T_{2,adi} + T_2}{2} \right) \tag{3.15}$$

where k is the thermal conductivity of the fluid. L_{char} is an characteristic linear dimension, in the case of a compressor it is the external case diameter. The temperature used is the difference between the wall temperature, T_{ch} and the mean value of the adiabatic outlet temperature of the compressor, $T_{2,adi}$ and the measured outlet temperature, T_2. $\overline{Nu}$ is the Nusselt number which describes the ratio of convective to conductive heat transfer.
The Nusselt number is defined by the equation

$$\overline{Nu}_{t\to th} = c_0 Re^{c_1} Pr^{c_2} \left(\frac{\mu_{bulk}}{\mu_{skin}} \right)^{c_3} \tag{3.16}$$

where the constants c_0 to c_3 differs depending on the used model, Re is the Reynolds number, and Pr is the Prandtl number.

The Reynolds number describes the condition of the flow where low values represent a flow that is mostly laminar while high numbers indicates that the flow is mostly turbulent.
The Reynolds number is defined by

$$Re = \frac{\rho u L_{char}}{\mu} = \frac{u L_{char}}{v} \tag{3.17}$$

where ρ is the density of the fluid, u its velocity, and μ, v the dynamic and kinematic viscosity of the fluid.
The Prandtl number is the ratio of viscous diffusion rate to thermal diffusion rate and is defined by the equation,

$$Pr = \frac{c_p \mu}{k} \tag{3.18}$$

where c_p is the heat capacity for air at constant pressure. Since $c_{p,air}$ differs with the temperature of the air, a model from Cengel et al. (2017) were used where;

$$c_{p,air} = A_0 + A_1 T + A_2 T^2 + A_3 T^3 \tag{3.19}$$

are used to calculate the specific heat of the air. The constants used in equation (3.19) are shown in Table 3.1.

Compressor

The dimensionless calculation of heat transfer in the compressor is defined in Serrano et al. (2015) as,

$$\overline{Nu}_{ch\to c} = \begin{cases} 0.284 Re^{0.8} Pr^{0.3} & \text{if} \quad Q < 0 \\ 0.095 Re^{0.8} Pr^{0.4} & \text{if} \quad Q > 0 \end{cases} \tag{3.20}$$

Table 3.1: *Values of constants for calculation of specific heat of air.*

Constant	Value
A_0	28.11
A_1	0.1967 e-2
A_2	0.4802 e-5
A_3	-1.96 e-9

which is a parameterized version of equation (3.16) used specifically for the compression.

Turbine

The same calculations can be made on the turbine side but here the heat is transferred from the gas to the wall and the equations for the Nusselt number differs compared to the compressor equation. In Eriksson (2002) the Nusselt equation is written as in equation (3.16). The constants are shown in Table 3.2 where some are standard and some developed specifically to exhaust systems.

Table 3.2: *Values of constants for calculation of Nusselt number (Eriksson, 2002).*

Correlation	c_0	c_1	c_2	c_3
CatonHeywood	0.258	0.8	0	0
Shayler1997a	0.18	0.7	0	0
SiederTate	0.027	0.8	1/3	0.14
WendlandTakedown	0.081	0.8	1/3	0.14
WendlandTailpipe	0.0432	0.8	1/3	0.14
Malchowetal	0.0483	0.783	0	0
meisnerSorenson	0.0774	0.769	0	0
DOHCDownpipe	0.26	0.6	0	0
ValenciaDownpipe	0.83	0.46	0	0
PROMEX	0.027	0.82	0	0
Woods	0.02948	0.8	0	0
Blair	0.02	0.8	0	0
Standard	0.01994	0.8	0	0
std_tu	0.023	0.8	0.3	0
Eriksson	0.48	0.5	0	0
std_lam1	1.86	1/3	1/3	0.14
Reynolds	0.00175	1	0	0

Table 3.3: *Values of constants for calculation of specific heat ratio for exhaust gases.*

Constant	Value
a_1	0.692
a_2	39.17 e-6
a_3	52.9 e-9
a_4	-228.62 e-13
a_5	277.58 e-17
b_0	3049.33
b_1	-5.7 e-2
b_2	-9.5 e-5
b_3	21.53 e-9
b_4	-200.26 e-14

3.1.5 Polynomial calculation of the specific heat ratio, γ

The specific heat ratio, γ can be calculated by using a polynomial model of internal energy at combustion of iso-octane and deriving it with respect to the temperature. Using the model developed by Krieger and Borman the specific heat ratio can be described as

$$\gamma_{KP} = \frac{c_p}{c_v} = 1 + \frac{R}{c_v} \tag{3.21}$$

where R is the specific gas constant for the burnt mixture of air and iso-octane. c_v is the heat capacity at constant volume and is defined as

$$c_v = \frac{\partial u}{\partial T} \tag{3.22}$$

where u is the internal energy, so by calculating the specific gas constant,

$$R(T, p, \lambda) = 0.287 + \frac{0.020}{\lambda} + R_{corr}(T, p, \lambda) \tag{3.23}$$

and using it in the equation for internal energy,

$$u(T, p, \lambda) = A(T) - \frac{B(T)}{\lambda} + u_{corr}(T, p, \lambda) \tag{3.24}$$

where $A(T)$ and $B(T)$ are polynomials which have the form,

$$\begin{aligned} A(T) &= a_1 T + a_2 T^2 + ... + a_5 T^5 \\ B(T) &= b_0 + b_1 T + ... + b_4 T^4 \end{aligned} \tag{3.25}$$

The values for the constants in (3.25) are found in Table 3.3. The terms u_{corr} and R_{corr} are non-zero first when T > 1450 K which will make them zero for all tests done on the turbine in this thesis.

4

Heat transfer model

This section will describe the implementation of the proposed heat model. The heat transfer model used in this thesis will rely on a node type of model, each node are capable of heat transfer through convection, radiation and conduction. Heat transfer between nodes are only possible through conduction. The turbocharger are split into three nodes, the assumption made is that the difference in enthalpy drop in the turbine, and the enthalpy gain in the compressor, is equal to all losses that occurs in between. The three nodes that the turbocharger are divided into includes turbine housing, bearing housing and compressor housing. The model equations in this chapter are only valid during stationary operation, where energy in to the system equals energy out of the system.

4.1 Turbine

The total enthalpy drop in the Turbine is assumed to consist of only heat transfers and work. From the first law of thermodynamics the energy flows in the turbine gas control volume are described by

$$\dot{Q}_{conv_{t\to th}} = \dot{m}_t C_{p_t}(T_3 - T_4) - W_t \tag{4.1}$$

Turbine housing

The turbine housing have heat transfer in four different directions. Convection from the exhaust gases, convection to ambient, radiation to ambient, and conduction to bearing housing. This is described in the following equation,

$$\dot{Q}_{conv_{t\to th}} + \dot{Q}_{rad_{th\to amb}} + \dot{Q}_{conv_{th\to amb}} + \dot{Q}_{cond_{th\to bh}} = 0 \tag{4.2}$$

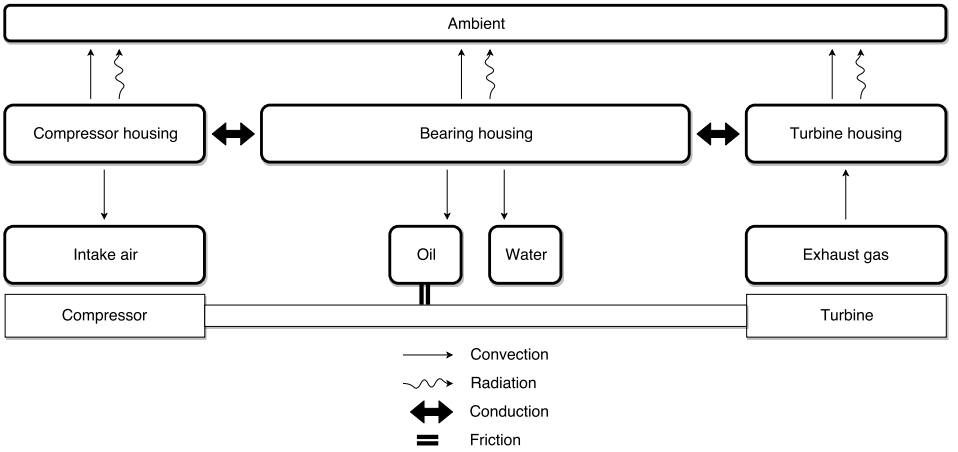

Figure 4.1: *Overview of the heat model with three nodes. All nodes are connected through conduction, each node can transfer heat through radiation, convection and conduction.*

where positive flow is directed to the turbine housing, and where each of the heat transfers are described by,

$$\dot{Q}_{rad_{th\to amb}} = \sigma \epsilon_x A_{th} T_{th,surf}^4 \tag{4.3}$$

$$\dot{Q}_{conv_{th\to amb}} = h_{th} A_{th} (T_{th,surf} - T_{amb}) \tag{4.4}$$

$$\dot{Q}_{cond_{th\to bh}} = A_{tb} k_{tb} (T_{th} - T_{tb}) \tag{4.5}$$

Bearing housing

The bearing housing receives heat from the turbine housing. Heat is transferred through convection to oil, water, and ambient. Also, heat is radiated from the bearing housing to the ambient, and heat is transferred through conduction to the compressor backplate. The expression for all heat transfers in the bearing housing is given by

$$\dot{Q}_{cond_{th\to bh}} + \dot{Q}_{oil} + \dot{Q}_{wtr} + \dot{Q}_{rad_{bh\to amb}} + \dot{Q}_{conv_{bh\to amb}} + \dot{Q}_{cond_{bh\to ch}} = 0 \tag{4.6}$$

where positive flow is directed to the bearing housing, and where each of the heat transfers are described by,

$$\dot{Q}_{oil} = \dot{m}_{oil} C_{p_{oil}} (T_{oil_{in}} - T_{oil_{out}}) \tag{4.7}$$

$$\dot{Q}_{wtr} = \dot{m}_{wtr} C_{p_{wtr}} (T_{wtr_{in}} - T_{wtr_{out}}) \tag{4.8}$$

$$\dot{Q}_{rad_{bh\to amb}} = \sigma \epsilon_x A_{bh} T_{bh,surf}^4 \tag{4.9}$$

$$\dot{Q}_{conv_{bh\to amb}} = h_{bh} A_{bh} (T_{bh,surf} - T_{amb}) \tag{4.10}$$

$$\dot{Q}_{cond_{bh\to ch}} = A_{cb} k_{cb} (T_{cb} - T_{ch}) \tag{4.11}$$

Compressor housing

The compressor housing have essentially the same heat transfers as the turbine housing. Heat is conducted from the bearing housing to the compressor housing, convection occurs between the housing and ambient/intake air, and radiation emits from the surface of the compressor housing to ambient. The thermal relations are given by,

$$\dot{Q}_{cond_{bh\to ch}} + \dot{Q}_{rad_{ch\to amb}} + \dot{Q}_{conv_{ch\to amb}} + \dot{Q}_{conv-_{ch\to c}} = 0 \tag{4.12}$$

where positive flow is directed to the compressor housing, and each heat transfer can be described by,

$$\dot{Q}_{rad_{ch\to amb}} = \sigma \epsilon_x A_{ch} T_{ch,surf}^4 \tag{4.13}$$

$$\dot{Q}_{conv_{ch\to amb}} = h_{ch} A_{ch} (T_{ch,surf} - T_{amb}) \tag{4.14}$$

$$\dot{Q}_{conv_{ch\to c}} = \underbrace{\frac{1 - e^{\frac{-h_{cv}A_c}{\dot{m}_c C_{p_c}}}}{\frac{-h_{cv}A_c}{\dot{m}_c C_{p_c}}} h_{cv}}_{h_{g_{comp}}} A_c (T_{ch} - T_2) \tag{4.15}$$

Compressor

The total enthalpy gain in the Compressor are assumed to consist of only heat transfers and work. From the first law of thermodynamics the energy flows in the compressor gas control volume are described by

$$\dot{Q}_{conv_{ch\to c}} = \dot{m}_c C_{p_c} (T_2 - T_1) - \dot{W}_c \tag{4.16}$$

4.2 Calculation of models

Since the amount of measured quantities in a regular engine are nowhere near the amount measured in the engine test bench, the resulting models would preferably have to be reliant on those few quantities that are measured in a regular engine to be useful in a real world scenario. All models will therefore be a function of one or a combination of air mass flow, exhaust mass flow, engine torque and engine speed. Polynomial or exponential functions with various degrees will be fitted to measured data to receive the models. The polynomial function is given by,

$$f(x) = \sum_{k=0}^{n} a_k x^{n-k} \tag{4.17}$$

and the exponential function is given by,

$$f(x) = a \cdot e^{bx} + c \cdot e^{dx} \tag{4.18}$$

5

Measurements

In this section many of the practical aspects of the measurements are described. Placement of sensors on the turbocharger, test equipment specifications, testing method, as well as the tested operating points of the engine.

5.1 Test setup

The test setup hardware consists of a turbocharger prepared with a number of thermocouple and pressure sensors. Figure 5.1 shows the position of the sensors located on the surface, Figure 5.2 shows the rest of the temperature and pressure sensors which includes gas, fluid and ambient temperatures and pressures. In Table 5.6, the corresponding numbers and description of the sensors are explained.

5.1.1 Testing method

Temperature measurements are done at steady state, this is reached by having a constant throttle angle at a desired load point. Various temperatures, and varying pressure ratios are tested with different load points, these are found in the quick reference guide, Table 5.1. After about ten minutes the temperatures over the turbocharger are stabilised. At steady state all the measured temperatures and pressures are recorded for ten seconds, the mean value of these recordings are then used in the calculations of heat transfer. When the sampling is done the rpm and load is changed to the next in the list and the process repeated. This is done at all desired test points with variations in test setup, wastegate at 24, and 100% open, insulation of compressor and lastly with the turbine also insulated.

Table 5.1: *Quick reference guide for speed and load during tests. Δ means that the operating point is done insulated and uninsulated. All operating points are done with wastegate at 0, 24 and 100% open.*

Speed \ Load	15 [Nm]	20 [Nm]	35 [Nm]	55 [Nm]	95 [Nm]	110 [Nm]	135 [Nm]
1000 [RPM]	X	X	Δ	X	Δ	X	Δ
1500 [RPM]	X	X	Δ	X	Δ	X	Δ
2000 [RPM]	X	X	Δ	X	Δ	X	Δ
2500 [RPM]	X	X	Δ	X	Δ	X	Δ
3000 [RPM]	X	X	Δ	X	Δ	X	Δ
3500 [RPM]	X	X	Δ	X	Δ	X	Δ

5.1.2 Hardware

A few different variations of each type of sensor will be used. This section will give general information and important specifications of each sensor used.

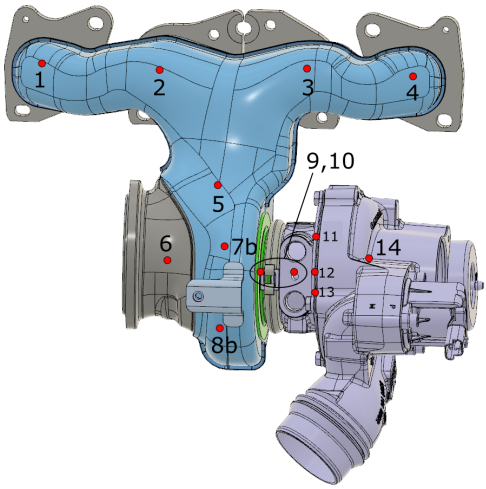

Figure 5.1: *Sensor placement for all surface temperature sensors on the turbocharger and exhaust manifold, the sensor list is shown in Table 5.6.*

The finished turbocharger preparation is shown in Figure 5.3 where most of the thermocouple sensors are visible. Also visible in the figure are the wires by which the sensors are connected to the thermoscanner. In Figure 5.4 a closeup on the turbine housing show 7a, an inner wall sensor and the surface temperature sensors 7b and 9 which are welded to the surface. Also, the figure show 21, the

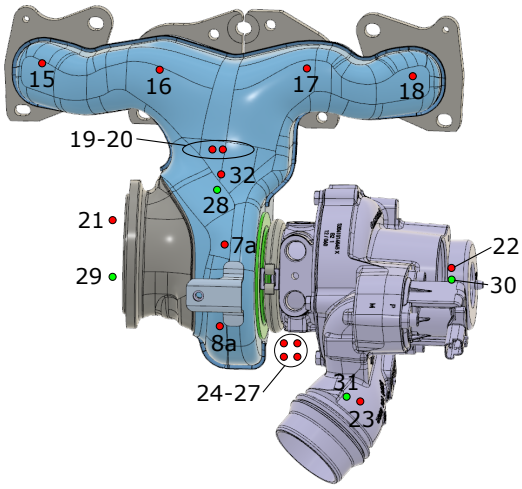

Figure 5.2: *Sensor placement for all temperature sensors excluding surface temperature sensors, the sensor list is shown in Table 5.6. Temperature sensors are shown as red dots, pressure sensors are shown as green dots.*

gas temperature after turbine, and 29 the nipple for the pressure sensor after turbine. The gas temperature is measured in the centre of the flow as shown in Figure 5.5. To measure the gas temperature before the turbine a hole is drilled and the sensor is inserted to the centre of the flow as shown in Figure 5.6.

Thermocouples

The thermocouples are used to measure all temperatures on the turbocharger, except the surface temperatures. The manufacturer of the sensors are Pentronic. Technical specifications are shown in Table 5.2. Two variants of this thermocouple will be used, one with insulated measuring junction, and one with exposed measuring junction. The exposed variant have faster dynamics, but shorter life span.

Table 5.2: *Thermocouple specifications*

Property	**Value**
Max temp	1200 °C
Diameter	1.5/3.0 mm
Metal sheath	Inconel 600

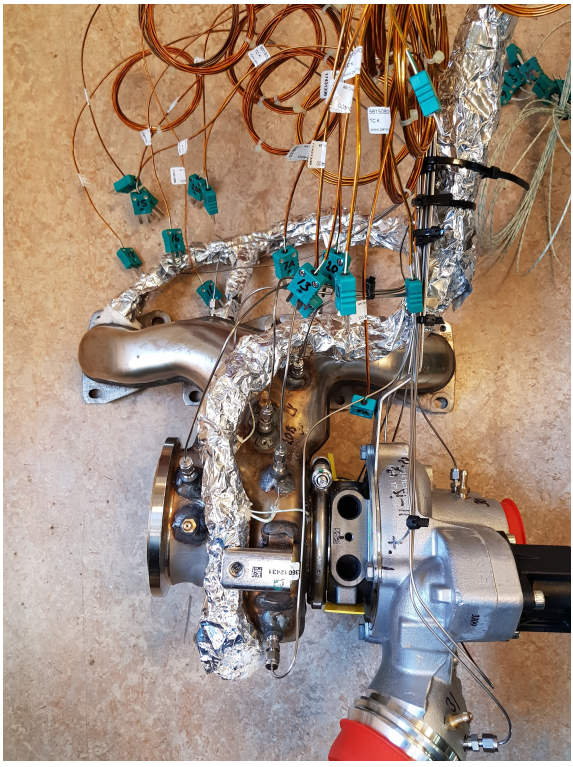

Figure 5.3: *The finished turbo prep with most of the thermocouple sensors showing.*

Flow sensor

The flow in the turbocharger coolant will be measured. The name of the sensor used is FT-110 made by Gems Sensors. The sensor uses the Hall Effect to measure the flow throughput, a turbine inside the sensor rotates when a flow is passing through. A certain amount of revolutions of the turbine will correspond to a total amount of flow. In Table 5.3 the technical specifications of the sensor is shown.

Table 5.3: *Flow rate sensor specifications*

Property	**Value**
Flow range	2-35 l/min
Pulses per litre	700
Frequency output	23-408 Hz
Operating temperature	-20°C to 100°C
Accuracy	±3% of reading
Repeatability	0.5% of full scale

Figure 5.4: *Closeup on the turbine housing where sensors 7a, 7b, 9, 21, and 29 are marked with red circles.*

Insulation material

In order to eliminate certain heat fluxes, in particular the surface radiation, an insulation material is used. The chosen material is a type of mineral wool that can withstand the temperatures of the turbocharger without losing its function.

5.1.3 Material data

The turbochargers different parts are made with different materials. This is a short explanation of what specific properties the materials of the outer and inner walls of the exhaust manifold, the turbine housing, bearing housing, and compressor housing have.

Exhaust manifold and Turbine

The exhaust manifold is dual layered where the outer wall, turbine housing, and exhaust pipes are all cast from stainless steel 1.4828, while the inner wall are made from stainless steel 1.4571. The Turbine scroll is made from stainless steel 1.4848. One thing to note is that the thermal properties in Table 5.4 and 5.5 are given at 20°C. No information were found in a higher range of temperatures for these specific materials, although for similar materials these properties do rise with temperature.

The main characteristics are shown in Table 5.4 where it is noted that the materials do not differ much.

Figure 5.5: *Compressor outlet where the gas temperature sensor, 23 is shown to be centred in the gas flow.*

Table 5.4: *Material data for the exhaust manifold*

Property	**Inner wall** [1.4571]	**Outer wall/housing** [1.4828]	**Turbine scroll** [1.4848]
Density	8 $[g/cm^3]$	7.9 $[g/cm^3]$	7.8 $[g/cm^3]$
Thermal Conductivity @20°C	15 [W/m K]	15 [W/m K]	15 [W/m K]
Specific heat Capacity @20°C	500 [J/kg K]	500 [J/kg K]	490 [J/kg K]

Bearing and Compressor housing

The bearing housing is made of the material EN-GJL-250, which is a common grey cast iron. The compressor housing are made with AC-AlSi11Cu2(Fe) which is an aluminium alloy. The material data is shown in Table 5.5.

Table 5.5: *Material data for the bearing/compressor housing*

Property	**Compressor housing** [AC-AlSi11Cu2(Fe)]	**Bearing housing** [EN-GJL-250]
Density	2.7 $[g/cm^3]$	7.2 $[g/cm^3]$
Thermal Conductivity @20°C	47 – 80 [W/m K]	204 [W/m K]
Specific heat Capacity @20°C	89 [J/kg K]	460 [J/kg K]

Figure 5.6: Turbine inlet cross-section showing how the gas temperature sensor is centred in the gas flow.

5.2 Tests

Two test scenarios were planned, one in the gas stand at VCC and one in the test bench at Linköping university. The gas stand tests were never done but are still included in this part to indicate how they would have been done. The turbocharger used is a single turbo aimed for gasoline engines. For the gas stand tests the turbocharger would have been prepped with an extension on the turbine outlet that separated wastegate flow from the turbine flow, enabling mass flow measurements through the wastegate.

5.2.1 Gas stand tests

Since it is not possible to separate the flow through the wastegate from the turbine during regular operation this needs to be done in the gas stand. In most applications today the mass flow through the wastegate is calculated by comparing the boost pressure when the wastegate is not fully closed to tests where the wastegate was kept closed and all of the flow went through the turbine. The exhaust mass flow through the wastegate is then calculated by subtracting the calculated turbine mass flow from the total exhaust mass flow.

In this thesis a more direct way of estimating the flow through the wastegate is attempted by using a model where the position of the wastegate and engine data is used to calculate the mass flow. The wastegate can be modelled as a valve opening to a larger volume, enabling the use of choked flow equations

To calculate the effective area of the flow past the wastegate, tests would have to be done where the mass flow is separated from the turbine flow by some sort of solution, earlier tests in cold conditions have used a welded pipe directly onto the exhaust side of the wastegate to separate the flow and enable measurement. The position of the electrical servo is then used as a reference for how the wastegate is

positioned, since the exact position of the wastegate is not measured. During the tests the wastegate position α is set in positions varying from fully closed to fully open. Doing this at different pressure ratios Π, and temperatures T_u, enables the model during steady state to be described as,

$$\dot{m}_{wg} = A_u \rho_u \eta_u = A_d \rho_d \eta_d \tag{5.1}$$

$$\dot{m} = \frac{p_u}{\sqrt{RT_u}} A_{eff}(\alpha) \Psi_{cv} \quad \Leftrightarrow \quad A_{eff}(\alpha) = \frac{\dot{m}\sqrt{RT_u}}{p_u \Psi_{cv}} \tag{5.2}$$

$$\Psi_{cv}(\Pi) = \sqrt{\frac{\gamma+1}{2\gamma}(1-\Pi)\left(\Pi + \frac{\gamma-1}{\gamma+1}\right)} \tag{5.3}$$

One of the downsides with doing gas stands tests are the differences compared to a real combustion engine. The pulsating flow is removed, and if the exhaust mass flow is to be measured through both wastegate and turbine it is required to separate them with different collector volumes. A result of this is among other things different pressure drops over the wastegate and turbine, which may lead to a bad model estimation of the flow.

5.2.2 Engine test bench

The test bench located at Vehicular Systems at Linköping University is equipped with a gasoline engine from the Volvo VEA engine family.

The tests were focused around getting data on how the surface, gas, and fluid temperatures across the turbocharger changed with different load points.

By isolating the compressor or changing the flow of cooling water the amount of heat transferred to the air in the compressor can be changed. In doing so at the same engine speeds and load points as done earlier the thermal quantity can be altered and measured so that when combined with the equation (4.1) the difference give.

Case 1: Insulated compressor.

$$\dot{Q}_{cond_{bh\to ch},iso} + \dot{Q}_{rad_{ch\to amb},iso} + \dot{Q}_{conv_{ch\to amb},iso} + \dot{Q}_{conv_{ch\to c},iso} = 0 \tag{5.4}$$

Case 2: Uninsulated compressor.

$$\dot{Q}_{cond_{bh\to ch}} + \dot{Q}_{rad_{ch\to amb}} + \dot{Q}_{conv_{ch\to amb}} + \dot{Q}_{conv_{ch\to c}} = 0 \tag{5.5}$$

If equation (5.5) are subtracted by equation (5.4), with the assumption that convection and radiation to ambient are negligent in the isolated case, the following equation are given,

$$\Delta\dot{Q}_{conv_{ch\to c}} + \sigma \epsilon_{ch} A_{ch} T_{ch,surf}^4 + h_{ch} A_{ch} (T_{ch,surf} - T_{amb}) = 0 \tag{5.6}$$

where if σ, A_{ch}, ϵ_{ch}, and h_{ch} are assumed to be constant during steady state it can be simplified to

$$\Delta\dot{Q}_{conv_{ch\to c}} + C_{1,ch}T_{ch,surf}^4 + C_{2,ch}(T_{ch,surf} - T_{amb}) = 0 \tag{5.7}$$

enabling the compressor work to be be calculated by modelling the amount of heat transfer at different load points.

The same test but with isolation of the turbine housing will enable same calculations for the turbine side,

Case 1: Insulated turbine.

$$\dot{Q}_{conv_{t\to th},iso} + \dot{Q}_{cond_{th\to bh},iso} + \dot{Q}_{rad_{th\to amb},iso} + \dot{Q}_{conv_{th\to amb},iso} = 0 \tag{5.8}$$

Case 2: Uninsulated turbine.

$$\dot{Q}_{conv_{t\to th}} + \dot{Q}_{cond_{th\to bh}} + \dot{Q}_{rad_{th\to amb}} + \dot{Q}_{conv_{th\to amb}} = 0 \tag{5.9}$$

If equation (5.9) are subtracted by equation (5.8), with the assumption that convection and radiation to ambient are negligent in the isolated case, the following equation are given,

$$\Delta\dot{Q}_{conv_{t\to th}} + \sigma\epsilon_{th}A_{th}T_{th,surf}^4 + h_{th}A_{th}(T_{th,surf} - T_{amb}) = 0 \tag{5.10}$$

where once again the area of the turbine housing can be estimated and the emissivity, ϵ_{th} is a material dependant constant. This enables the simplified equation,

$$\Delta\dot{Q}_{conv_{th\to c}} + C_{1,th}T_{th,surf}^4 + C_{2,th}(T_{th,surf} - T_{amb}) = 0 \tag{5.11}$$

Table 5.6: *Placement and description of the sensors attached to the turbocharger.*

Measurement	Number	Description
Surface temperature	1	Exhaust port 1
	2	Exhaust port 2
	3	Exhaust port 3
	4	Exhaust port 4
	5	Turbine inlet
	6	Turbine outlet
	7b	Turbine housing 1
	8b	Turbine housing 2
	9	Turbine backplate
	10	Bearing housing
	11	Compressor backplate 1
	12	Compressor backplate 2
	13	Compressor backplate 3
	14	Compressor housing
Gas temperature	15	Exhaust port 1
	16	Exhaust port 2
	17	Exhaust port 3
	18	Exhaust port 4
	19	Exhaust pipe 1
	20	Exhaust pipe 2
	32	Before turbine
	21	After turbine
	22	Before compressor
	23	After compressor
Inner wall temperature	7a	Turbine, Inner wall 1
	8a	Turbine, Inner wall 2
Oil temperature	24	Oil before
	25	Oil after
Water temperature	26	Water before
	27	Water after
Pressure sensors	28	Before turbine
	29	After turbine
	30	Before compressor
	31	After compressor

6
Results

In this chapter the results of the tests shown in section 5 are presented. The parameters required for the models are estimated and validated versus the experimental data. All models and figures in this chapter are produced with tests where the wastegate was closed, unless stated otherwise.

6.1 Internal heat transfer

In the sections below the result of the transfer of heat from the exhaust gases to the turbine housing, and the heating of the intake air from the compressor housing, as well as the internal conduction between nodes are shown.

6.1.1 Compressor work and heat transfer

To calculate the compressor work and efficiency the usage of dimensionless numbers, shown in section 3.1.4, were used together with temperatures sampled on the compressor housing, and air temperatures before and after the compressor. The resulting temperatures compared to the mass flow of air are shown in Figure 6.1. It is shown that for all of the load points the compressor housing is cooler than 90°C and that the difference between compressor housing and gas temperature is quite small during low mass flows. For low loads, $\dot{m}_{air} < 20$ [g/s], air temperature after the compressor is lower than that of the compressor housing, meaning that heat is transferred from the housing to the air. During high loads however, $\dot{m}_{air} > 30$ [g/s], the air temperature after the compressor can reach levels higher than the compressor housing. This means that the heat transfer will be reversed, the compressor house is now being warmed by the compressed air. By comparing the calculated heat transfer with the enthalpy gain, the amount of

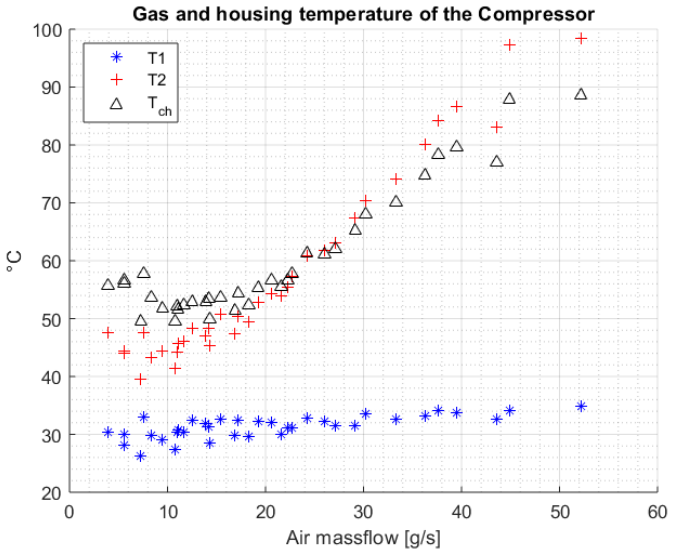

Figure 6.1: *The temperatures of T1, T2, and T_{ch} compared to the mass flow of air past the compressor. At flows > 30 [g/s] the compressor housing temperature is lower than T2 reversing the flow of heat.*

compressor work can be estimated.

$$W_{comp} = \Delta H_{comp} - \dot{Q}_{nusselt} \tag{6.1}$$

In Figure 6.2 the calculated heat transfer using Nusselt numbers, as shown in equation (3.15), from the compressor housing to the intake air is shown together with the enthalpy gain over the compressor and the calculated compressor/turbine power. Interesting to note is that for low flows the amount of heat transferred to the air is almost all of the enthalpy gain while for higher mass flows it falls of, showing that the compressor efficiency increases with air massflow. This is to expect as said earlier in the report, the compressor efficiency increases with compressor speed. The compressor efficiency is estimated by,

$$\eta_{comp} = \frac{W_{comp}}{\Delta H_{comp}} \tag{6.2}$$

and plot of this is shown in Figure 6.3. The efficiency of the compressor is plotted for three wastegate positions versus the amount of air mass flow. Since the opening of the wastegate is not measured the position of the servo, were 0 is fully closed and 100 is fully open, is used to describe how much the wastegate is open. It is shown that with the wastegate closed the compressor is working more adiabatic at higher speeds and that the efficiency is very low at low speeds. With open wastegate the efficiency is even negative during very low speeds, showing that the compressor can be viewed as a resistance to the flow.

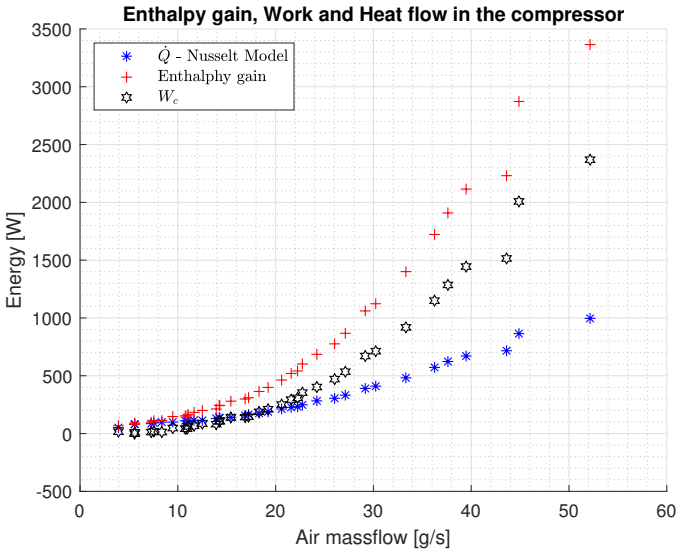

Figure 6.2: *The calculated gain in enthalpy over the compressor is shown together with the calculated heat transfer and compressor power. The compressor efficiency is very low at low air massflows.*

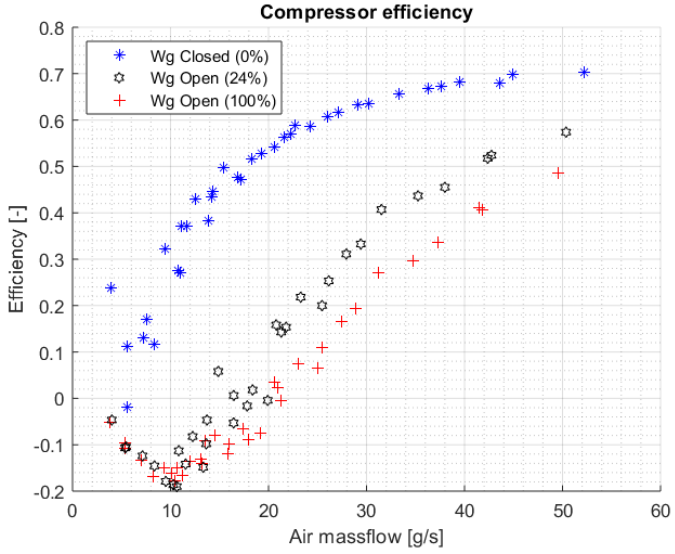

Figure 6.3: *Compressor efficiency for three wastegate servo positions, 0% are fully closed, 100% are fully open. With the wastegate open no work is done to the air and P2<P1 for flows under 20 [g/s]. The compressor can in this case be viewed as a resistance to the flow and thus giving negative values in the plot.*

6.1.2 Turbine work and heat transfer

On the turbine side the heat flows from the heated exhaust gases to the inner wall of the turbine housing. To calculate the heat transfer and the effectiveness of the turbine the temperatures before and after expansion were measured together with the inner, and outer wall temperatures. The turbine temperatures are plotted in Figure 6.4 were the the gas temperatures before, and after the turbine are shown together with the mean housing, and the inner wall temperature versus the amount of exhaust gas mass flow. As can be seen in the figure the temperature difference between T3 and T4 is not very large when the gas flow is low. Another observation is that there exists multiple operating points where there are different temperatures at the same amount of gas flow for flows under 25 [g/s]. This can be explained by the fact that two or more operating points have the same amount of gas flow.

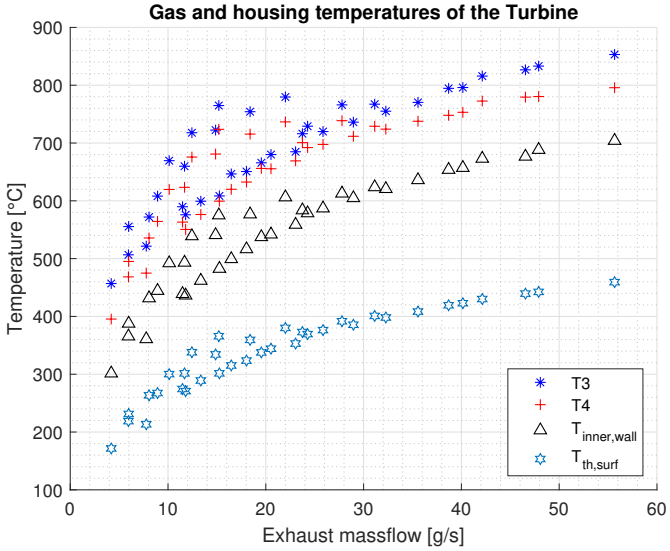

Figure 6.4: *Gas temperatures T3 and T4 together with inner and outer wall temperatures for closed wastegate plotted against the amount of exhaust gas mass flow. Flows below 25 [g/s] contains multiple operating points with different temperatures but close to equal gas flow.*

Since the turbine and compressor are connected by a shaft, and the friction on it is assumed to be low enough to be neglected, the assumption can be made that the work done by the exhaust gases on the turbine are the same that the compressor delivers to the intake air. Using this assumption it is possible to use the enthalpy drop over the turbine, equation (3.3) and the calculated work done by the compressor, equation (6.1) to estimate the amount of heat transferred from the exhaust gases to the turbine housing as,

$$\dot{Q}_{turb} = \Delta H_{turb} - W_{comp} \tag{6.3}$$

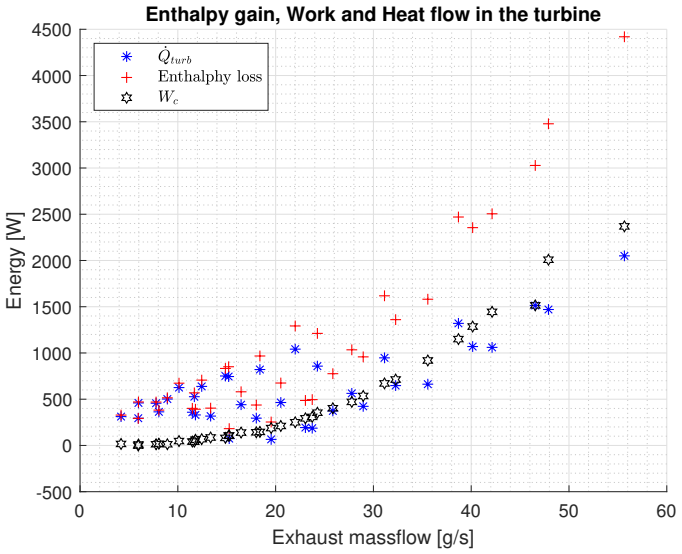

Figure 6.5: *Enthalpy drop over the turbine shown together with the calculated work done by the compressor and the difference between them being the heat loss.*

Equation (6.3) could then be used to calculate the efficiency of the turbine as,

$$\eta_{turb} = \frac{W_{comp}}{\Delta H_{turb}} \tag{6.4}$$

In the Figure 6.5 the enthalpy drop over the turbine, calculated using the first law of thermodynamics (3.2), is shown together with the calculated compressor work, and the difference between them. This figure is quite a lot messier then the one on the compressor but the trend is the same. During low flows almost all of the enthalpy drop is heat losses, and at higher speeds the turbine works more efficient and for flows over 40 [g/s] the amount of work surpasses calculated amount of heat losses.

The amount of heat transferred to the turbine housing from the exhaust gases can also be calculated with dimensionless numbers as shown in equation (3.16). The turbine side is far more complicated compared to the compressor, with temperatures differing by hundreds of degrees and the geometry between engines and turbochargers contributing to how the heat transfer is modelled. To try to find a fitting model all 17 different cases shown in Table 3.2 were tried together with the above mentioned calculated heat loss to try to find some model that matches. The result is shown in Figure 6.6 where the closest match is the Caton-Haywood model though it is still a bad fit compared to the calculated heat loss. This indicates that for this engine and exhaust a new model with different parameters needs to be created.

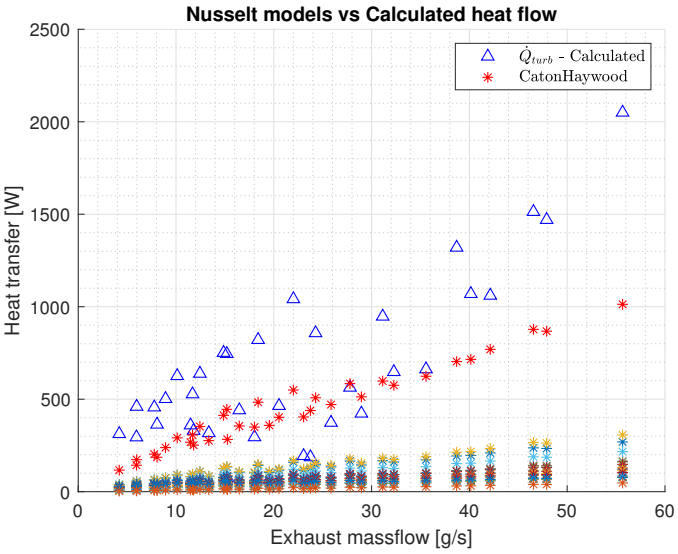

Figure 6.6: *The 17 different Nusselt models for heat transfer shown in Table 3.2 together with the estimated heat transfer, from measured data in blue, to the turbine housing vs gas mass flow. The closest model, CatonHaywood is marked in red.*

6.1.3 Heat transfer between nodes

Internal heat transfer between the turbine, bearing, and compressor housing is assumed to be entirely done by conduction. By measuring the differences in temperature between the insulated and non insulated tests the difference in heat flow can be calculated.

Compressor and bearing housing

The compressor housing was insulated using mineral wool to investigate the amount of heat transfer to the compressor housing. The heat transferred to the compressor housing is split in two parts, radiation from hot surfaces and by convection from the surrounding air. By comparing the enthalpy gain from the original, uninsulated test to the isolated one a difference can be measured. Using the same operating points the assumption is made that the only difference between the tests should be the external heat transfer. In Figure 6.7 the compressor backplate, and bearing housing temperatures are plotted versus the amount of air mass flow. Notable is that with the compressor insulated the temperature of the bearing housing remains constant but the compressor backplate becomes cooler for flows between 25-40 [g/s]. A larger difference in temperature brings with it a higher amount of heat flow from the bearing housing to the compressor housing.

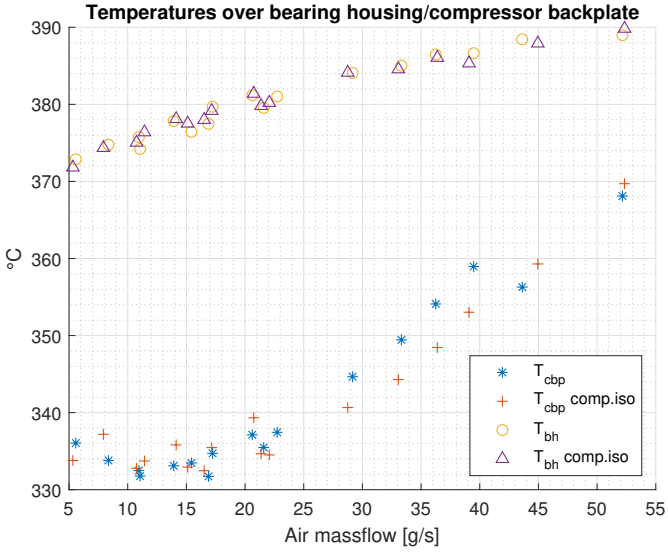

Figure 6.7: *Compressor backplate and bearing housing temperatures for the uninsulated and insulated tests. The lowering of compressor temperature increases the conductive heat flow between the parts.*

The difference in heat transfer can be described by the equations,

$$\text{Case 1: } \dot{Q}_{comp,1} = \dot{Q}_{cond_{bh\to ch,1}} + \dot{Q}_{rad} + \dot{Q}_{conv,1} + \dot{Q}_{conv_{ch\to c,1}} \tag{6.5a}$$

$$\text{Case 2: } \dot{Q}_{comp,2} = \dot{Q}_{cond_{bh\to ch,2}} + \dot{Q}_{conv,2} + \dot{Q}_{conv_{ch\to c,2}} \tag{6.5b}$$

where Case 1 is non insulated and Case 2 is insulated. The variable $\dot{Q}_{cond_{bh\to ch}}$ is the conduction heat transfer between the bearing housing and the compressor housing. The variables $\dot{Q}_{conv,1/2}$ is the amount of convection from the bearing housing to the ambient air. With no forced convection done during tests, convection heat transfer to the ambient is deemed low and lower for the insulated case, $\dot{Q}_{conv,1} > \dot{Q}_{conv,2}$, but not much can be said about their absolute value.

Since there is no way to exactly measure the conductive heat transfer between two different materials this will be treated as an unknown and contribute to the error of the model. What can be said about the conductive heat transfer is that it is larger when the temperature difference between bearing, and compressor housing is larger. The difference in heat transfer can be expressed by the function,

$$\Delta\dot{Q}_{cond_{bh\to ch}} = f(\Delta T) \tag{6.6}$$

where ΔT is the difference in temperature between the bearing, and compressor housings.

The variables $\dot{Q}_{conv_{ch\to c,1/2}}$ are representing the amount of heat transfer from the compressor housing to the intake air. This is calculated with the dimensionless numbers shown in equation (3.20) and visualised in Figure 6.8. As shown the

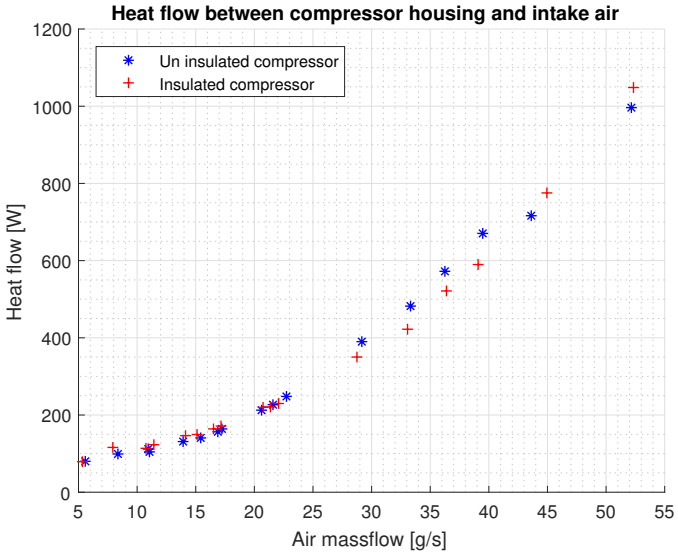

Figure 6.8: *Calculated heat flow between the compressor housing and intake air for the insulated and uninsulated tests. The small difference indicates that not a large amount of heat is transferred from the ambient or the bearing housing.*

difference in calculated heat exchange between the compressor housing and the intake air is relatively small with the insulation of the compressor. The maximum measured difference in heat transfer is 17% and the mean absolute percentage difference is under 8% when calculated by,

$$M = \frac{100}{N} \sum_{i=1}^{N} \left| \frac{\dot{Q}_{conv_{ch\to c,1,i}} - \dot{Q}_{conv_{ch\to c,2,i}}}{\dot{Q}_{conv_{ch\to c,1,i}}} \right| = 7.9396\% \tag{6.7}$$

Considering the assumptions made above, the heat transfer on the compressor side can be said to mostly depend on the heat transfer between compressor housing and intake air, treating the heat transfer from the bearing housing and from the ambient as noise. The compressor heat transfer model can then be created as a function of the enthalpy gain over the compressor, and the efficiency of the compressor,

$$\dot{Q}_{comp} = (1 - \eta_{comp})\Delta h_{comp} + \dot{Q}_{error} \tag{6.8}$$

Turbine and bearing housing

By insulating the whole turbo, including the turbine, bearing housing and compressor, in mineral wool external radiation and convection is removed or at least considered small enough to neglect. By comparing the isolated vs the uninsulated tests the difference in enthalpy can be said to be the effect that is lost in heat transfer to the ambient. In Figure 6.9 the turbine and bearing housing temperatures are plotted versus the amount of exhaust gas mass flow. Notable is that with the whole turbocharger insulated the temperature of the bearing housing remains constant but the turbine housing increases in temperature which in turn leads to a larger difference in temperature between the two. A larger difference in temperature brings with it a higher amount of heat flow from the turbine housing to the bearing housing. The difference in heat transfer can be described by

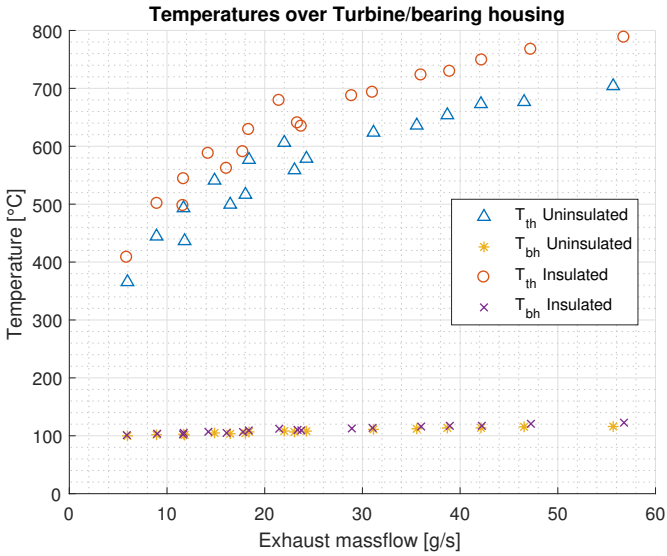

Figure 6.9: *Turbine housing and bearing housing temperatures for the uninsulated and insulated tests. The increase of turbine temperature increases the conductive heat flow between the parts.*

the equations,

$$\text{Case 1: } \dot{Q}_{turb,1} = \dot{Q}_{cond_{th\to bh,1}} + \dot{Q}_{rad} + \dot{Q}_{conv,1} + \dot{Q}_{conv_{t\to th,1}} \tag{6.9a}$$

$$\text{Case 2: } \dot{Q}_{turb,2} = \dot{Q}_{cond_{th\to bh,2}} + \dot{Q}_{conv,2} + \dot{Q}_{conv_{t\to th,2}} \tag{6.9b}$$

where Case 1 is non insulated and Case 2 is insulated. The variables $\dot{Q}_{conv,1/2}$ are the amount of convection from the turbine housing to the ambient air. In the lab the airflow past the turbine is very low compared to how it is in a car, where a fan or the speed of the car forces air past the turbine. With almost no flow of air the convection heat transfer to the ambient is deemed quite low and even lower

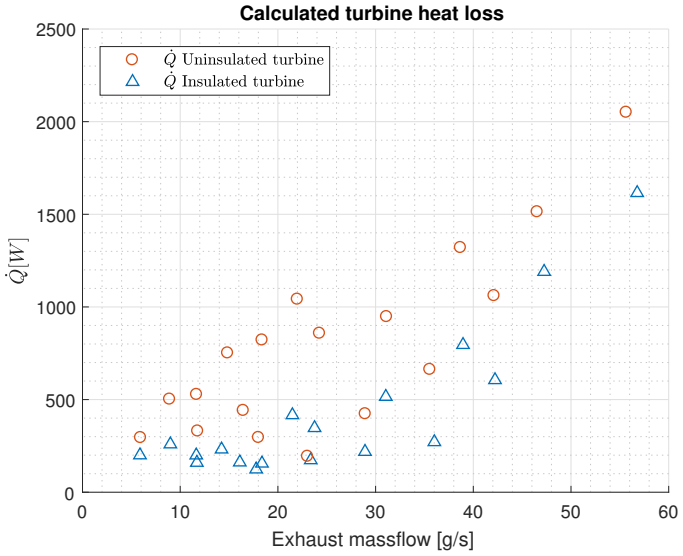

Figure 6.10: *Difference in calculated heat transferred from the exhaust air to the turbine housing versus the exhaust gas mass flow. When insulated the heat loss from the exhaust gases to turbine wall decreases for all mass flows.*

for the insulated case, $\dot{Q}_{conv,1} > \dot{Q}_{conv,2}$, but not much can be said about their absolute value.

The variable $\dot{Q}_{cond_{th\to bh}}$ is the conduction heat transfer between the turbine housing and the bearing housing. Since there is no way to exactly measure the conductive heat transfer between two different materials this will be treated as an unknown and contribute to the error of the model. What can be said about the conductive heat transfer is that it is larger when the temperature difference between turbine, and bearing housing is larger. The difference in heat transfer can be expressed by the function,

$$\Delta\dot{Q}_{cond_{th\to bh}} = f(\Delta T) \tag{6.10}$$

where ΔT is the difference in temperature between the turbine, and bearing housings.

The variables $\dot{Q}_{conv_{t\to th,1/2}}$ are representing the amount of heat transfer from the exhaust gases to the turbine housing. This is calculated with equation (6.3) and visualised in Figure 6.10. As shown in the figure the difference in calculated heat exchange between the exhaust gas and turbine housing lessens by insulating the turbine. Since the work done by the compressor is still the same for all work points, the efficiency of the turbine calculated as shown in equation (6.4) increases. This is shown in Figure 6.11

It is observed in Figure 6.12 that the heat transfer to the engine coolant are almost identical when the compressor and whole turbocharger are insulated.

Considering the results above, the heat transfer on the turbine side can be said to mostly depend on the heat transfer between exhaust gases and and housing. The heat transfer from the turbine housing to bearing housing is not especially affected by the insulation of the turbo. The turbine heat transfer model can then be calculated as a function of the difference in enthalpy over the turbine and the efficiency of the turbine,

$$\dot{Q}_{turb} = (1 - \eta_{turb})\Delta h_{turb} + \dot{Q}_{error} \tag{6.11}$$

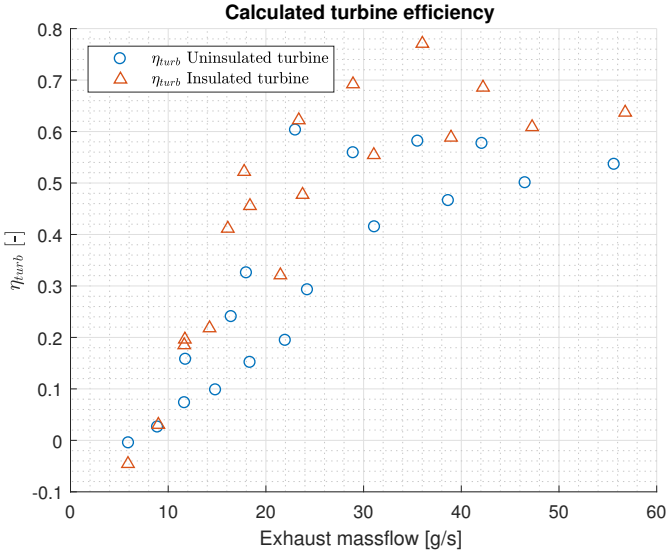

Figure 6.11: *Difference in calculated turbine efficiency between insulated and uninsulated turbine. By insulating the turbine the efficiency is increased for all mass flows.*

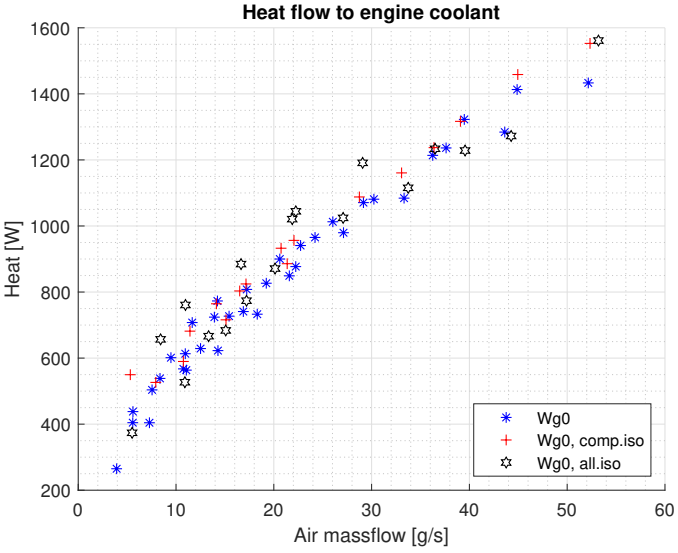

Figure 6.12: *Heat transferred to engine coolant for three different conditions, normal, compressor insulated, and whole turbocharger insulated.*

6.2 Calculation of model parameters

To build a model of the turbo efficiency and heat transfer the results presented above is used to parameterize the constants used in the models. All constants used in the model are shown in Table 6.1. The models are estimated using certain operating points in a set of data, they are then evaluated on all available operating points in that set of data. The operating points for the evaluation data are given in Table 5.1 as triangles.

6.2.1 Compressor

Starting at the compressor, the equation for the compressor efficiency is built as,

$$\hat{\eta}_{comp}(\dot{m}_{air}) = C_1\dot{m}_{air}^3 + C_2\dot{m}_{air}^2 + C_3\dot{m}_{air} + C_4 \tag{6.12}$$

the resulting model is shown in Figure 6.15 where the data points and model is shown together.

Using the same approach as in equation (6.12) the enthalpy gain over the compressor is modelled considering the mass flow as,

$$\Delta\hat{h}_{comp}(\dot{m}_{air}) = C_1\dot{m}_{air}^3 + C_2\dot{m}_{air}^2 + C_3\dot{m}_{air} + C_4 \tag{6.13}$$

the resulting model is shown in Figure 6.13 where the data points and model is shown together.

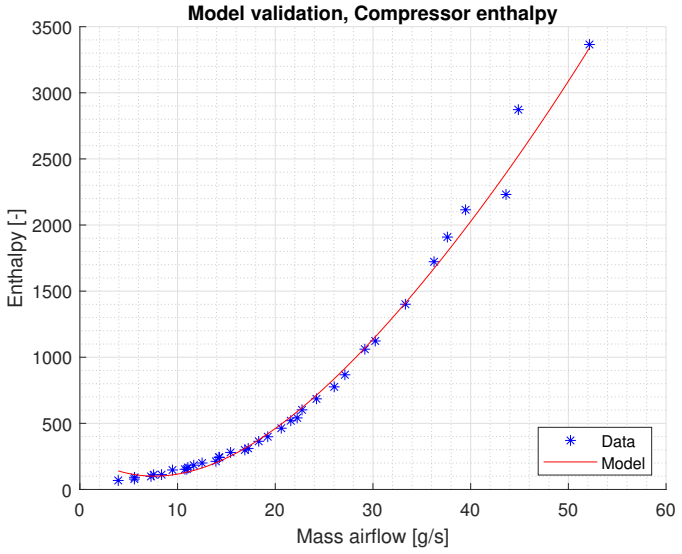

Figure 6.13: *Model validation for the compressor enthalpy, the model follows the measured data well across the whole range except for two operating points during high air massflow.*

Using the calculated model for compressor efficiency, and the model for enthalpy gain it is possible to estimate the the amount of heat transfer from just the mass flow past the compressor.

$$\dot{\hat{Q}}_{comp} = (1 - \hat{\eta}_{comp})\Delta\hat{h}_{comp} \tag{6.14}$$

which gives us the heat loss model shown in Figure 6.14 where the model is shown beside the calculated heat loss done above with dimensionless numbers.

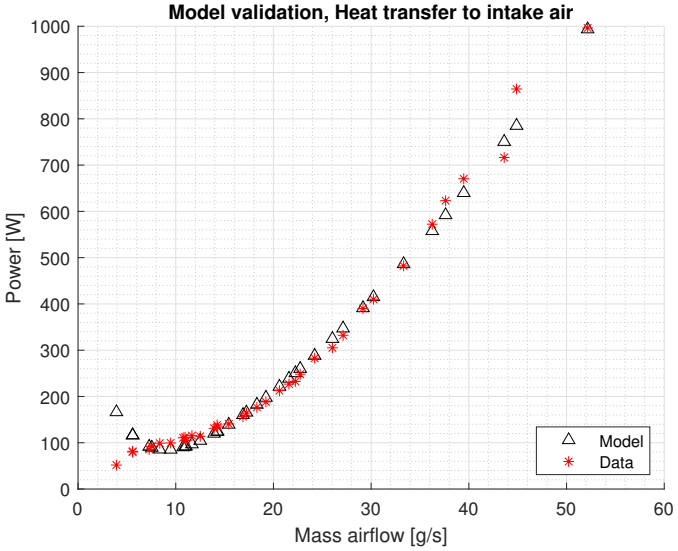

Figure 6.14: *Model validation for the heat transfer from compressor housing to intake air, the model follow the measured data well except for a couple of operating points with low mass airflow.*

The maximum measured difference in heat transfer between the modelled values and calculated is 221% and the mean absolute percentage difference is under 14.5% when calculated by,

$$M = \frac{100}{N}\sum_{i=1}^{N}\left|\frac{\dot{Q}_{comp,nusselt} - \dot{\hat{Q}}_{comp}}{\dot{Q}_{comp,nusselt}}\right| = 14.493\% \tag{6.15}$$

The efficiency model for the Compressor is shown in Figure 6.15. The model utilizes a exponential function to estimate the efficiency satisfactory. The maximum measured difference in efficiency between the model and the data are 177% when the flow is low. The mean absolute percentage difference is under 17.1% as shown by,

$$M = \frac{100}{N}\sum_{i=1}^{N}\left|\frac{\eta_{comp} - \hat{\eta}_{comp}}{\eta_{comp}}\right| = 17.085\% \tag{6.16}$$

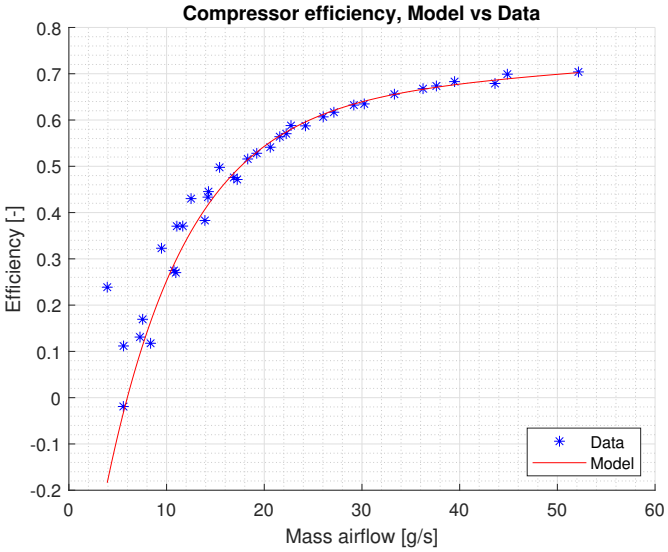

Figure 6.15: *Model validation of Compressor efficiency. The model uses an exponential function to estimate the efficiency, the accuracy are better during high loads.*

6.2.2 Bearing housing

In the bearing housing most of the external heat flow is to the cooling water. This heat flow can be described by the model

$$\dot{\hat{Q}}_{wtr} = C_1 \dot{m}_{air}^2 + C_2 \dot{m}_{air} + C3 \tag{6.17}$$

and is shown in Figure 6.16 where the data points and model is shown together.

The maximum measured difference in heat transfer between the modelled values and calculated is 35.4% and the mean absolute percentage difference is below 5.5% when calculated by,

$$M = \frac{100}{N} \sum_{i=1}^{N} \left| \frac{\dot{Q}_{wtr} - \dot{\hat{Q}}_{wtr,model}}{\dot{Q}_{wtr}} \right| = 5.4018\% \tag{6.18}$$

6.2.3 Turbine

At the turbine, the measured data are more scattered compared to the compressor data. The heat transfer from exhaust gases to turbine housing are calculated using the enthalpy drop over the turbine combined with the model for compressor work.

The nusselt model mentioned in section 3.1.4 is used and fitted to measured data using custom parameter values with inspiration from Table 3.2. The param-

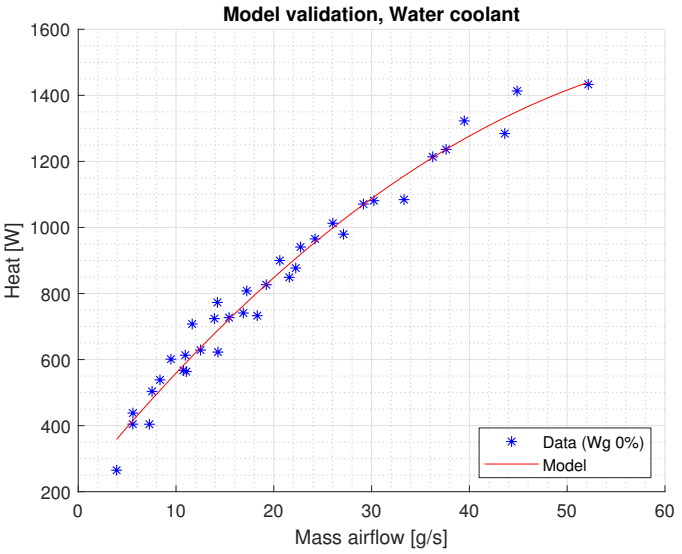

Figure 6.16: *Model validation of the heat flow to Water coolant, consistent data enables the model to be fairly accurate across all operating points.*

eters and model are given by the equation,

$$\overline{Nu}_{t\to th} = 0.4Re^{0.8}Pr^{0}\left(\frac{\mu_{bulk}}{\mu_{skin}}\right)^{0} = 0.4Re^{0.8} \tag{6.19}$$

and the heat transfer $\dot{Q}_{turb}$ is then calculated as in equation (3.15). A different model of the heat flow depending on the exhaust massflow were also produced, it is based on the data from the nusselt model given in (6.19). The heat flow model is given by:

$$\dot{\hat{Q}}_{turb}(\dot{m}_{air}) = a \cdot e^{b\dot{m}_{exh}} + c \cdot e^{d\dot{m}_{exh}} \tag{6.20}$$

Figure 6.17 shows the model validation for the turbine heat flow model, together with the measured data and nusselt model. A mean absolute percentage difference were calculated to 89% as shown by,

$$M = \frac{100}{N}\sum_{i=1}^{N}\left|\frac{\dot{Q}_{turb} - \dot{\hat{Q}}_{turb,nusselt}}{\dot{Q}_{turb}}\right| = 89\% \tag{6.21}$$

Models dependent on Rpm and Torque

The second approach to model turbine enthalpy and heat flow takes a few more parameters into consideration. It was found that the turbine enthalpy correlates to both engine speed and engine torque that enabled a more accurate model.

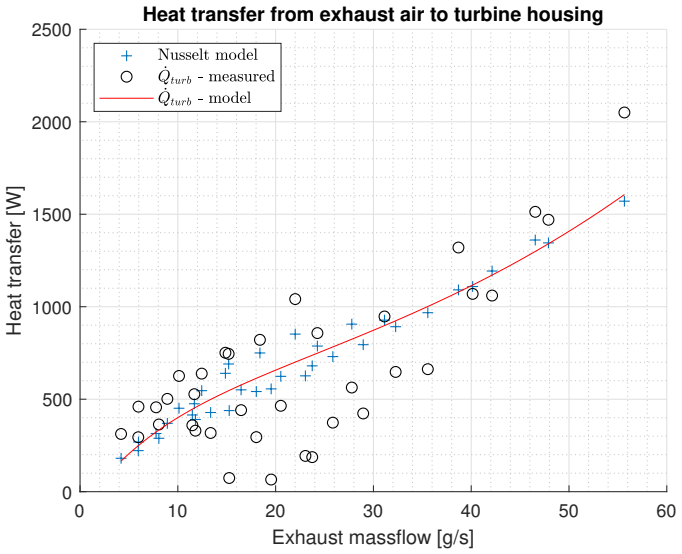

Figure 6.17: *Model validation of the heat flow from exhaust gases to turbine housing using the model based on the Nusselt-model. The model are best during high loads, but still not very accurate.*

Figure 6.18 shows the normalized enthalpy model on which the Heat flow model in Figure 6.19 are based. It was modelled by fitting a 4:th degree polynomial to the data provided by multiplying enthalpy, Rpm and Torque, depending on exhaust massflow. The polynomial model is given by,

$$Model = f(\dot{m}_{exh}) = C_1\dot{m}_{exh}^4 + C_2\dot{m}_{exh}^3 + C_3\dot{m}_{exh}^2 + C_4\dot{m}_{exh} + C_5 \tag{6.22}$$

and the enthalpy drop by,

$$\Delta h_{turb} = \frac{f(\dot{m}_{exh})}{Tq \cdot Rpm} \tag{6.23}$$

The mean absolute percentage difference for the normalized heat model were calculated to be 56%, a substantial improvement compared to the heat model based on the Nusselt model which received a 89 % mean absolute percentage difference.

$$M = \frac{100}{N}\sum_{i=1}^{N}\left|\frac{\dot{Q}_{turb} - \dot{\hat{Q}}_{turb,norm}}{\dot{Q}_{turb}}\right| = 56\% \tag{6.24}$$

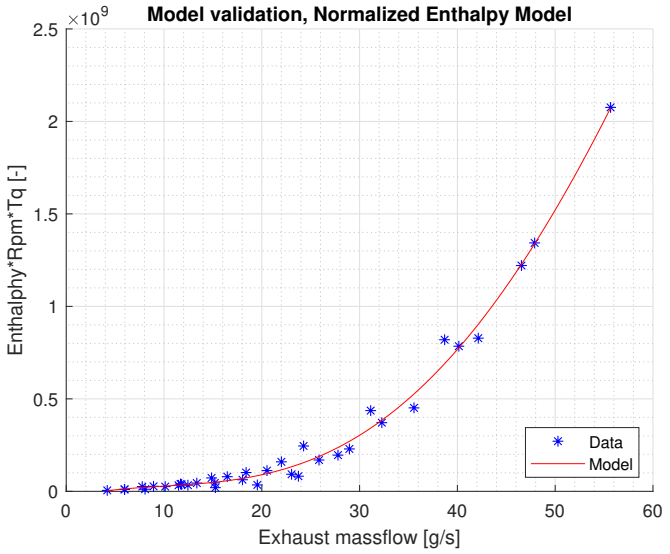

Figure 6.18: *Model validation of the normalized enthalpy model with Rpm and Torque dependency. The normalized enthalpy data shows a clear trend, compared to when only enthalpy were used.*

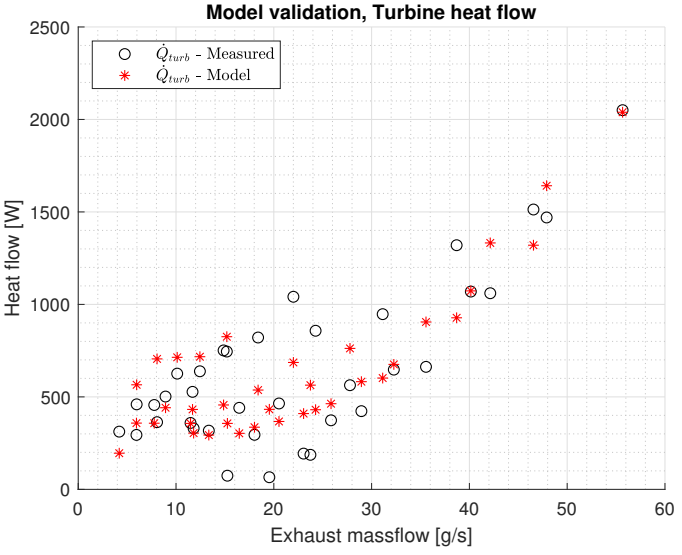

Figure 6.19: *Model validation of the heat flow from exhaust gases to turbine housing using the normalized enthalpy model. This model accuracy are a big improvement compared to the heat transfer model based on the nusselt-model in 6.17.*

Table 6.1: *Parameters for the models using polynomial and exponential estimations, equation* (4.17) *and* (4.18) *shows the function expressions.*

Polyfit models	C_1	C_2	C_3	C_4	C_5
$\hat{\dot{Q}}_{wtr}$ (6.17)	-0.2502	36.44	219.4	-	-
$\Delta\hat{h}_{comp}$ (6.13)	0.0003	-0.04594	3.727	-49.23	279.1
$f(\dot{m}_{exh})$ (6.22)	-242.3	4.059e+4	-1.069e+6	1.344e+7	-3.739e+7
Exp. models	a	b	c	d	-
$\hat{\eta}_{comp}$ (6.16)	0.6357	0.00198	-1.325	-0.1208	-
$\hat{\dot{Q}}_{turb,nusselt}$ (6.20)	441.6	0.0232	-540.2	-0.1239	

7

Discussion

This sections contains discussions about most aspects of this thesis. The model, measurements, implementation and results are topics that will be discussed.

7.1 Planning and Implementation

The goal of this master thesis was to create a model for the heat flow for the turbocharger, as well as a model for how the mass flow past the turbine was affected by wastegate position and dynamic flow. Quite soon it was revealed that the planned tests in the gas stand at VCC where the separation of flow between wastegate and turbine would be measured were not going to happen. The lack of gas stand tests scrapped the idea of estimation of flow past the wastegate forcing the focus of the thesis to change towards including only the heat transfer model. The shift in focus meant that the thesis was dependant on only the tests done in the engine lab at LiU. The tests were planned to all be done before half time of the total time spent on the thesis, this would leave plenty of time to process and analyse the data and redo any failed tests or do extra tests if deemed necessary. The testing was delayed by five weeks due to delays in delivery of the right hardware. And when all tests for what was thought to be a closed wastegate it turned out that the electrical actuator did in fact not close all the way due to installation error. These delays forced the analysis of data way into the end of the writing of the report and little to no time was left to iterate the results or redo any desired tests. So the first conclusion is that when planning to do tests including hardware, plan more time for delays and errors in equipment. And when you are able to do tests, always do a cycle of tests at the start of testing that concludes that the engine is running as it should so that no time is spent sampling data that is not usable.

7.2 Heat flow model

The heat flow models produced are using the assumption that all heat flows across the turbocharger were one dimensional. Some heat flows neglected when making the model, could have been implemented to improve the result. They are: heat from the turbine blades to the shaft, conduction to/from catalytic converter, conduction to/from the engine block/exhaust manifold, and convection to the oil. The radiation heat emitted from the turbocharger are included in the model, but the radiation heat received from ambient influences (such as the engine block) are not taken into consideration. All these "shortcomings" of the model will turn out as model errors.

7.2.1 External heat transfer

While the internal heat transfer can be modelled and calculated by analysing the test data as done in the result section of the report, the external heat transfer is much more built on assumptions and can not be calculated with the same precision. On the hot side the heat transfer is directed from the turbine to the surroundings, while on the cold side the compressor housing is slightly warmer in temperature than ambient air, but colder than the surfaces around it, making the heat transfer to the compressor housing by radiation, but away from it with convection.

Compressor Housing

As shown above in Figure 6.8 the difference in heat flow between insulated and uninsulated compressor was low during all operating points. The decrease in temperature between uninsulated and insulated proofs that the net heat flow is positive to the compressor housing. The compressor housing is warmer than the surrounding air meaning that the heat transfer by convection to the ambient will be directed from the housing to the air. The decrease in temperature between uninsulated and insulated however shows that the net heat flow is positive to the compressor housing. This means that the heat transfer by radiation from the surrounding parts is higher than the outgoing radiation.

By dividing the radiation into two separate units, one for inflow of radiation and one for outgoing radiation the equation for heat transfer will be,

$$\dot{Q}_{ch\rightarrow amb} + \dot{Q}_{ch,conv} + \dot{Q}_{ch,rad} = 0 \tag{7.1}$$

where $\dot{Q}_{ch,rad,in} < \dot{Q}_{ch,rad,out}$, which makes it hard to formulate a model for the heat transfer on the form shown in equation (4.13) since the radiation inflow $\dot{Q}_{ch,rad,in}$ is dependant on surrounding temperatures not measured in the tests.

Turbine Housing

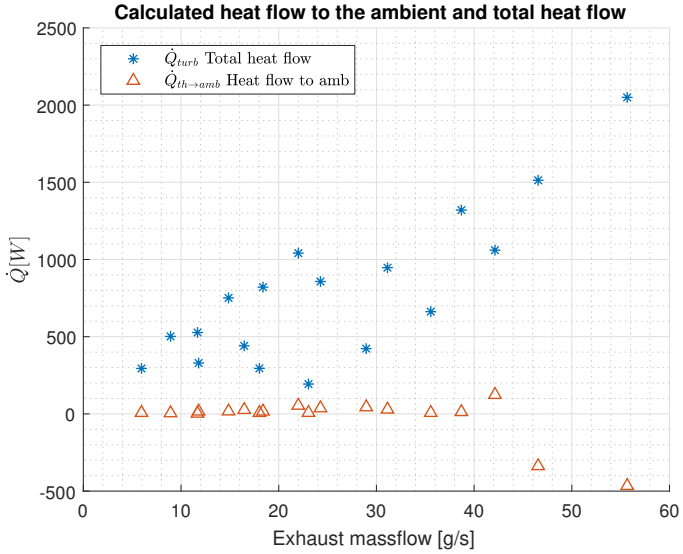

Figure 7.1: *The calculated amount of heat transfer to the ambient compared with total heat flow from the exhaust gases to the turbine inner wall. The plot shows that the net heat transfer to the turbine is close to zero for low flows and negative when the compressor is working more adiabatic during higher mass flows.*

On the hot turbine side the housing is hotter than the surrounding air making the convection work outwards. Due to the low amount of air flow past the turbine, no external fans are being directed at the turbine during testing, the majority of the heat transfer should be by radiation $\dot{Q}_{th,conv} < \dot{Q}_{th,rad}$. The temperatures difference between the turbine inner wall and exhaust gases decreases when insulated. A lower difference in temperature leads to the lower heat transfer shown already shown in Figure 6.10. The difference in heat transfer to the turbine wall subtracted from the difference in enthalpy drop for the insulated and uninsulated tests, shown in Figure 7.2, leaves us with the net heat flow to the ambient. This gives the equation to calculate the amount of heat flow to the ambient as,

$$\dot{Q}_{th\rightarrow amb} = \Delta h - \Delta h_{iso} - (\dot{Q}_{turb} - \dot{Q}_{turb,iso}) \tag{7.2}$$

The resulting heat transfer is shown in Figure 7.1, and indicates that the average amount of radiation and convection losses are very low during mass flows below 45 [g/s]. For higher mass flows, where the boost pressure starts to build and the turbine is working more adiabatic, the resulting heat flow is negative. This means that during high loads the net heat transfer is to the turbine housing from the ambient.

It seems unlikely that the net heat transfer during high loads would be directed to the turbine housing when it is almost 800°C warm. One of the factors that could explain this probably faulty result is how the system border is drawn. The system border is drawn where the turbine housing merges with the exhaust manifold and where it connects to the catalyst. The model does not include the heat transferred from the exhaust manifold to the turbine housing or the heat transferred to the catalyst, the assumption made was that they have similar temperatures. Another factor that comes into play during high temperatures is that the insulation gets warm on the outside and this leads to heat losses to the ambient that is not accounted for in the model.

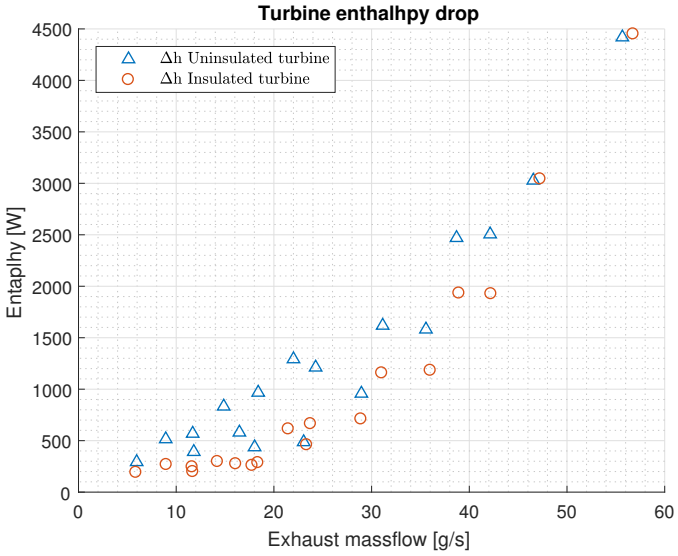

Figure 7.2: *Enthalpy drop over the turbine for the insulated and uninsulated tests versus exhaust gas mass flow.*

Bearing Housing

The main source of external heat transfer is the water cooling in the bearing housing. In the sections above it has been stated that close to no heat flows from the turbine housing to the ambient. This indicates that almost all of the heat should be transferred to the bearing housing and the cooling water. As shown in Figure 7.3 the enthalpy gain in the water past the bearing housing is equal to or bigger than the calculated heat loss in the turbine.

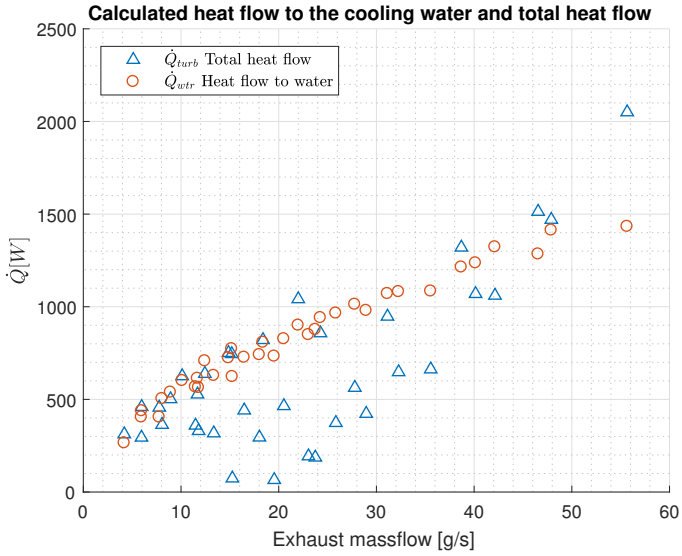

Figure 7.3: *Calculated heat loss in the turbine during non insulated test compared to the calculated heat transfer to the cooling water. It shows that the water is effectively doing all the heat transfer from the turbine.*

7.2.2 Model parameter estimation

In section 6.2 the model parameter estimation is presented. The reason why some of the polynomials are of the third and fourth degree are because some of the models depends on each other. The compressor enthalpy and efficiency models are used when estimating the compressor heat transfer model, when this calculation is made small errors in the enthalpy and efficiency model translates to a bigger error in the heat transfer model.

7.2.3 Turbocharger axle

The model used in the temperature calculations has several simplifications and assumptions. One of these simplifications includes the turbocharger turbine wheel, compressor wheel, and shaft. The heat transfer through these parts is ignored in the heat transfer model, this is the reason a sensitivity analysis is needed to determine the impact of this simplification.

A simple conductive heat transfer model was made with estimated parameters, constants from literature and datasheets. The model assumes that heat is transferred from the turbine wheel to the middle of the shaft. Figure 7.4 shows the shaft together with the length where heat transfer is considered, and the shaft diameter.

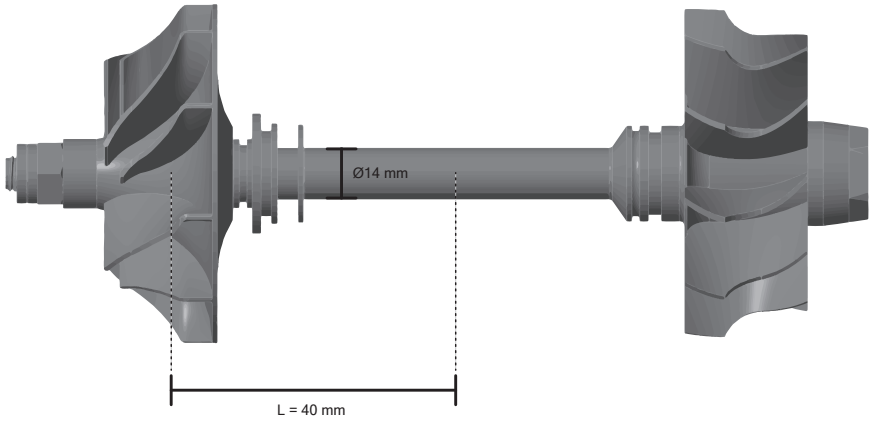

Figure 7.4: *Turbocharger shaft, turbine wheel, and compressor wheel.*

The heat transfer considered was 1D convective heat transfer. The temperature of the shaft closest to the turbine wheel was set to vary across a span of temperatures, the temperature closest to the compressor wheel was set to a constant of 80°C. Figure 7.5 shows the estimated heat flow through the turbocharger shaft during various start temperatures closest to the wheel. The result show that at most the turbo shaft could carry less then 70 [W] of heat to the water cooling with a temperature difference of 820°C.

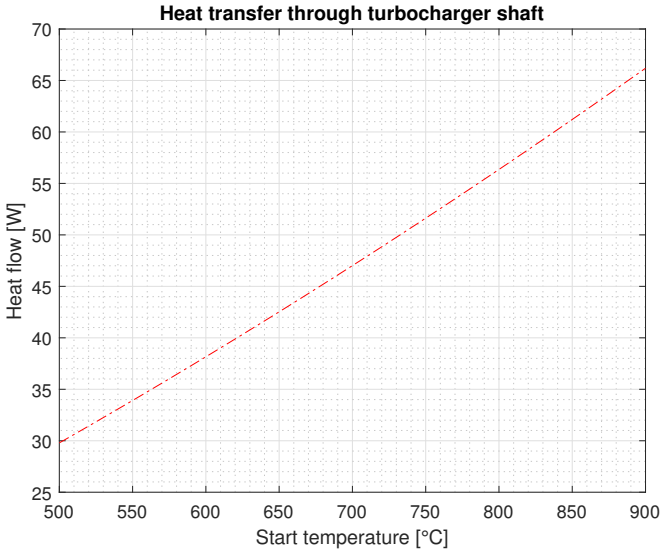

Figure 7.5: *Heat transferred through the turbocharger shaft vs the difference in temperatures of turbine and compressor housings.*

7.3 Measurements

The tests done, shown in Table 5.1, were concluded without any major breakdowns, the minor ones are discussed bellow.

7.3.1 Water flow

One of the uncertainties of the measurements on the engine are the amount of coolant flow the turbocharger actually receives. The first round of measurements, where most of the data were collected, displayed a constant water flow around 6.7 [l/min] in the turbo. During later stages of testing this flow changed to a lesser value. The function of the flow sensor could not be validated, which is why the water flow were assumed to be constantly 6.7 [l/min] across all measured operating points.

7.3.2 Temperature before turbine

During the measurements the temperature before the turbine, T3, were observed to measure unreasonable values. The temperature before would often be lower than the temperature after the turbine, T4. The solution to this problem was to use a mean of the two pipe-temperatures instead during calculations. A calibration test would have been preferred to validate the sensor.

7.3.3 Turbine enthalpy and heat transfer

The measured turbine enthalpy drop is quite messy where there exist multiple operating points with the same mass flow. This then extends when calculating the heat loss from exhaust gas to turbine wall since it is calculated as in equation (6.3).

In Figure 7.6 the calculated heat transfer dependent on gas flow is shown and the different test series are separated by torque, showing the problem with multiple test series having the same mass flow but different heat flow. This becomes hard to model since no apparent pattern can be found when looking only on the exhaust gas mass flow. Compare this with the same separation done on the compressor side in Figure 7.7 where a pattern is much easier to detect.

The parameterized Nusselt model shown in Figure 6.17 performs poorly compared to the model were the enthalpy was normalized with Rpm and torque and modelled as shown in Figure 6.19. When insulation is added to the turbocharger the difference in heat transfer at the same exhaust gas mass flow becomes much more compact, as shown in 6.10. To get a better model for heat transfer from the exhaust gases to the turbine wall it would be interesting to do more tests. One such test could be to add forced convection by directing a fan at the turbine during testing to see if the difference in heat flow lessens between operating points with the same mass flow, as seen when insulating.

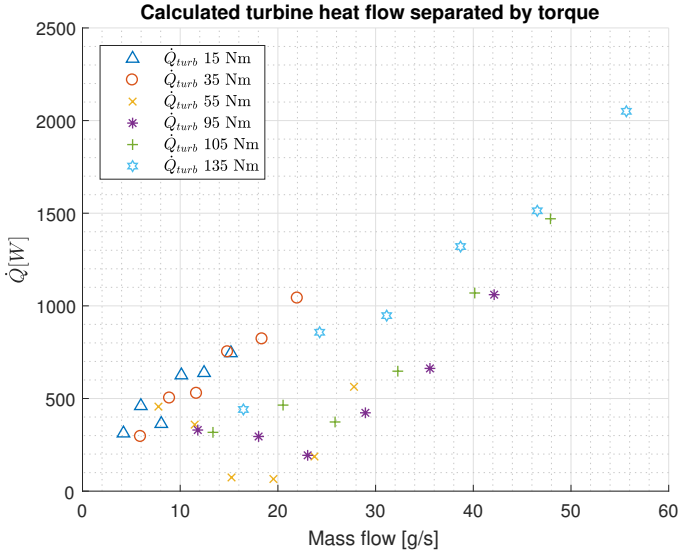

Figure 7.6: *Calculated heat transfer to the turbine wall from the exhaust gases, separated by torque. Different operating points have the same mass flow but different heat transfer.*

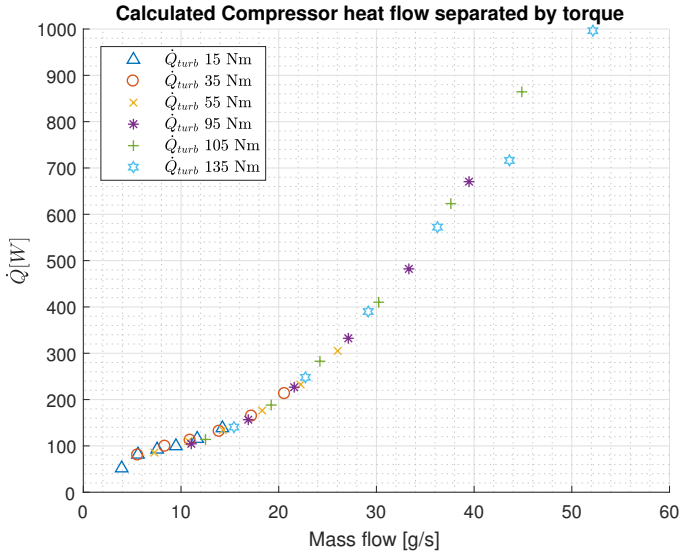

Figure 7.7: *Calculated heat transfer to the turbine wall from the exhaust gases, separated by torque. Different operating points have the same mass flow but different heat transfer.*

7.3.4 Insulation

The application of the insulation for the whole turbine and the compressor could be considered satisfactory, although the back side of the turbocharger were difficult to cover due to lack of space and visibility. During calculations the convection and radiation were assumed to be negligible when insulation were made, quite reasonable considering it was possible to put the hand on the insulation during testing, i.e the temperature difference to ambient was not that big.

7.3.5 Broken sensors

The surface mounted sensors were delicate and during the measurements, some of them broke. Fortunately, the sensors that broke had additional sensors close by that could be used instead with not much deviation.

7.4 Results

One of the main limitations of the results from this thesis is the hardware dependency of the models, conclusions can only be made for this particular engine with this particular turbocharger, the reason why are the many parameters and constants related to the engine and turbocharger.

The data collected shows that the compressor side have more consistent data when compared to the turbine side. For example, the enthalpy on the compressor side shows a much more consistent behaviour when plotted against air massflow, compared to the enthalpy on the turbine side when plotted against exhaust massflow. It was later found that the turbine enthalpy were greatly dependent on both engine speed and torque which improved the model accuracy. Overall the models on the compressor side were more accurate, this could be explained by the milder conditions around the compressor compared to the turbine. It doesn't need to deal with pulsating flow, exhaust gases and high temperatures etc.

As predicted, the water cooling of the turbocharger takes a big piece of the heat coming from the turbine. Figure 7.3 shows the heat flow of the cooling water compared to the heat flow from exhaust gases to turbine housing. One interesting note from this plot is the fact that the heat flow to the cooling water in many cases are higher than the heat flow from the exhaust gases to the turbine housing, according to our model this should be impossible. This leaves essentially two possibilities since the heat flow to water coolant is considered accurate. Either the calculated heat transfer in the turbine is inaccurate, or there are heat flow influences that the model doesn't consider.

8 Conclusions

In this chapter a summary of what the focus of the thesis has been and what results were reached are presented together with suggestions for future work.

8.1 Conclusions

The goal of this thesis was to improve the knowledge of how the heat transfer in the turbocharger can be described by models during low flows. To achieve this the turbo was divided into different nodes and a model was constructed for each of the nodes and the heat transfer between them. The implementation of these models were more successful on the compressor side where the flow is more homogeneous even during low mass flows, making the models fit quite good. On the hot turbine side the measurements during low loads are more sporadic and thus harder to model successfully. The models uses factors that can be measured in working conditions and this is a problem when the same mass flow is represented by different load points and temperatures on the turbine side. The magnitudes of the calculated heat transfers in the turbine, compressor and water coolant are all in the same range during the uninsulated tests, but the turbine heat transfer peaks the highest around 2 kW and the compressor heat transfer peaks the lowest at around 1 kW as can be seen in Figure 7.3 and 6.8.

Compressor

The conclusion of heat transfer is that the compressor side is quite insulated from the turbine. The data suggest that almost no heat is transported by conduction past the bearing housing and the water cooling. Heat that is transported to the compressor is mostly from the bearing housing. The water coolant and the bearing housing is warmer than the compressor housing and heat is transported be-

tween the two by conduction.

When looking at the interaction between the compressor and the ambient it does not seem as large as suggested by the related research. It was found that the insulation of the compressor made almost no difference to the intake air temperature or the compressor efficiency.

Turbine

The insulation of the turbine however showed a significant drop in how much enthalpy was lost over the turbine by decreasing the heat transfer to the turbine housing. This leads to an increase in its efficiency by quite a bit as shown in Figure 6.11.

Shaft and Oil

As shown in section 7.2.3 the amount of heat transferred by the shaft are negated since the estimated heat flow is so low. The heat transfer to the oil is also negated because of the sporadic flow and low delta temperature. This confirms the assumptions made by earlier work such as Serrano et al. (2015) where the amount of heat flow to the oil was shown to be negligible in the gas stand.

Models

The models showed good accuracy for the compressor heat flow, enthalpy, and the water coolant heat flow. The compressor efficiency model is not good at very low mass flows, this however seems to be more of an error in measurement rather than model error. The turbine side shows not that great results, the model for turbine enthalpy is not very good, although it got better after torque and engine speed were considered. One good thing about the models is that they are applicable during working conditions, they all depend on known quantities, but the downside is that the wastegate needs to be fully closed.

8.2 Future Work

The work done in this thesis could be expanded in many ways in the future, some of which are discussed below.

Material improvements

One of the uncertainties discovered in the work were that some of the sensors gave questionable measurements. The water flow sensor for example, showed inconsistent data during some tests. By changing to a better flow sensor the accuracy of this measurement could be increased. The same goes with the gas temperature sensor just before the turbine. In some tests it showed lower temperatures than after the turbine, which is unreasonable. New measurements with a working sensor, preferably a faster one, would be interesting.

Measurements on a real car could also be interesting. As discussed earlier the difference in air flow around the turbocharger is quite large when comparing a real car to the test bench, and to measure this difference would give data more relevant to the real application of the engine and therefor better models.

A more thorough insulation of the turbocharger is something that could benefit future tests, as of now the function of the insulation could not be verified enough to say that all convection and radiation were eliminated. The usage of radiation shields between components in the engine could increase the knowledge on how radiation from external components affect the turbocharger.

One interesting thing that might be applicable on a turbocharger are heat flux sensors, this would eliminate the need for material specific constants and coefficients.

Modelling

Since the gas stand tests were all abandoned, a model for the wastegate flow were difficult to produce, future work would include these tests to be able to estimate the flow.

The existing heat transfer model could also be improved by including more nodes into the heat transfer model. With more nodes more information is available, thus improving the resolution of the model, although this sets high standards on the equipment and preparations.

Bibliography

Habib Aghaali and Hans-Erik Angstrom. Improving turbocharged engine simulation by including heat transfer in the turbocharger. Technical report, SAE Technical Paper, 2012-01-0703, 2012. Cited on page 7.

Habib Aghaali, Hans-Erik Ångström, and Jose R Serrano. Evaluation of different heat transfer conditions on an automotive turbocharger. *International Journal of Engine Research*, 16(2):137–151, 2015. Cited on pages 5 and 6.

Nick Baines, Karl D Wygant, and Antonis Dris. The analysis of heat transfer in automotive turbochargers. *Journal of Engineering for Gas Turbines and Power*, 132(4):042301, 2010. Cited on page 6.

Dieter Bohn, Tom Heuer, and Karsten Kusterer. Conjugate flow and heat transfer investigation of a turbo charger. *Journal of engineering for gas turbines and power*, 127(3):663–669, 2005. Cited on page 6.

R Burke, P Olmeda, FJ Arnau, and MA Reyes-Belmonte. Modelling of turbocharger heat transfer under stationary and transient engine operating conditions. In *11th international conference on turbochargers and turbocharging*, volume 1384, page 103, 2014. Cited on page 7.

RD Burke, CRM Vagg, D Chalet, and P Chesse. Heat transfer in turbocharger turbines under steady, pulsating and transient conditions. *International Journal of Heat and Fluid Flow*, 52:185–197, 2015. Cited on page 7.

Yunus A Cengel, Robert H Turner, John M Cimbala, and Mehmet Kanoglu. *Fundamentals of thermal-fluid sciences*. McGraw-Hill New York, 5 edition, 2017. Cited on pages 10 and 13.

Mickaël Cormerais, Pascal Chesse, and Jean-François Hetet. Turbocharger heat transfer modeling under steady and transient conditions. *International Journal of Thermodynamics*, 12(4):193–202, 2009. Cited on page 7.

Lars Eriksson. Mean value models for exhaust system temperatures. Technical report, SAE Technical Paper, 2002-01-0374, 2002. Cited on page 14.

Lars Eriksson and Lars Nielsen. *Modeling and control of engines and drivelines*. John Wiley & Sons, 2014. Cited on page 5.

Robin Holmbom and Lars Eriksson. Analysis and development of compact models for mass flows through butterfly throttle valves. Technical report, SAE Technical Paper, 2018. Cited on page 11.

ISY. Software packages from vehicular systems, May 2018. URL `http://www.vehicular.isy.liu.se/en/Software/`. Cited on page 8.

Marcus Klein. *A specific heat ratio model and compression ratio estimation*. Division of Vehicular Systems, Department of Electrical Engineering, Linköping University, PhD Thesis, 2004. Cited on page 8.

Hung Nguyen-Schäfer. *Rotordynamics of automotive turbochargers*. Springer, 2016. Cited on page 5.

P Olmeda, V Dolz, FJ Arnau, and MA Reyes-Belmonte. Determination of heat flows inside turbochargers by means of a one dimensional lumped model. *Mathematical and computer modelling*, 57(7-8):1847–1852, 2013. Cited on page 7.

Francisco Payri, Pablo Olmeda, Francisco J Arnau, Artem Dombrovsky, and Les Smith. External heat losses in small turbochargers: Model and experiments. *Energy*, 71:534–546, 2014. Cited on page 6.

A Romagnoli and Ricardo Martinez-Botas. Heat transfer on a turbocharger under constant load points. In *ASME Conference Proceedings*, volume 48869, pages 163–174, 2009. Cited on pages 5 and 6.

Alessandro Romagnoli and Ricardo Martinez-Botas. Heat transfer analysis in a turbocharger turbine: An experimental and computational evaluation. *Applied Thermal Engineering*, 38:58–77, 2012. Cited on page 6.

José R Serrano, Pablo Olmeda, Francisco J Arnau, Miguel A Reyes-Belmonte, and Hadi Tartoussi. A study on the internal convection in small turbochargers. proposal of heat transfer convective coefficients. *Applied Thermal Engineering*, 89:587–599, 2015. Cited on pages 6, 13, and 62.

JR Serrano, P Olmeda, A Paez, and F Vidal. An experimental procedure to determine heat transfer properties of turbochargers. *Measurement Science and Technology*, 21(3):035109, 2010. Cited on page 6.

Borislav Sirakov and Michael Casey. Evaluation of heat transfer effects on turbocharger performance. *Journal of Turbomachinery*, 135(2):021011, 2013. Cited on pages 5 and 6.

Karl Storck, Matts Karlsson, Ingrid Andersson, Johan Renner, and Dan Loyd. *Formelsamling i termo- och fluiddynamik*. The Institute of Technology, Linköping University, December 2012. Cited on pages 9, 10, and 11.

Josefin Storm. Heat transfer modeling for turbocharger control. Master's thesis, Linköping University, 2017. Cited on pages 2, 5, and 7.

Giovanni Tanda, Silvia Marelli, Giulio Marmorato, and Massimo Capobianco. An experimental investigation of internal heat transfer in an automotive turbocharger compressor. *Applied Energy*, 193:531–539, 2017. Cited on page 6.

Carl Vilhelmsson. Compressible flow modeling with combustion engine applications. Master's thesis, Linköping University, 2017. Cited on pages 2 and 7.